THE RELATIVE STRENGTHENING OF STEELS AT HIGH STRAIN-RATES OF UNDERWATER EXPLOSIVE LOADING

James Walker Lisenby

and

John Elmer Rasmussen

Cambridge 39, Massachusetts

21 May 1956

Professor Leicester F. Hamilton
Secretary of the Faculty
Massachusetts Institute of Technology
Cambridge 39, Massachusetts

Dear Sir:

In accordance with the requirements of the degree of Naval Engineer, we herewith submit a thesis entitled "The Relative Strengthening of Steels at the High Strain-Rates of Underwater Explosive Loading."

Respectfully,

THE RELATIVE STRENGTHENING OF STEELS AT THE HIGH STRAIN-RATES OF UNDERWATER EXPLOSIVE LOADING

by

JAMES WALKER LISANBY, Lieutenant, U. S. Navy
B. S., U. S. Naval Academy, 1950

and

JOHN ELMER RASMUSSEN, Lieutenant, U. S. Navy
B. S., U. S. Naval Academy, 1947

SUBMITTED IN PARTIAL FULFILLMENT OF THE
REQUIREMENTS FOR THE DEGREE OF
NAVAL ENGINEER

at the
Massachusetts Institute of Technology
21 May 1956

Signature of Authors _____

_____

Certified by: _____
Thesis Supervisor

Accepted by: _____
Chairman, Departmental
Committee on Graduate
Students

THE RELATIVE STRENGTHENING OF STEELS AT THE HIGH STRAIN-RATES OF UNDERWATER EXPLOSIVE LOADING

by

JAMES WALKER LISANBY, Lieutenant, U. S. Navy
B. S., U. S. Naval Academy, 1950

and

JOHN ELMER RASMUSSEN, Lieutenant, U. S. Navy
B. S., U. S. Naval Academy, 1947

SUBMITTED IN PARTIAL FULFILLMENT OF THE
REQUIREMENTS FOR THE DEGREE OF
NAVAL ENGINEER

at the

Massachusetts Institute of Technology

21 May 1956

ACKNOWLEDGEMENTS

The authors wish to acknowledge the valuable assistance and guidance of: Lieutenant Commander H. E. Henning, USN; Dr. A. H. Kiel and Dr. H. M. Schauer of the Underwater Explosions Research Division, Norfolk Naval Shipyard, Portsmouth, Virginia; and Professor F. A. McClintock, Massachusetts Institute of Technology.

ABSTRACT

THE RELATIVE STRENGTHENING OF STEELS AT THE HIGH STRAIN-RATES OF UNDERWATER EXPLOSIVE LOADING

by

James W. Lisanby and John E. Rasmussen

Submitted to the Department of Naval Architecture and Marine Engineering on 21 May 1956 in partial fulfillment of the requirements for the degree of Naval Engineer.

The purpose of this investigation was to investigate the relative strengthening of steels resulting from the high strain rates resulting from underwater explosions. Steel plates of equal size and shape, but of different composition, were subjected to the same explosive loading. The energy absorbed by the plastic deformation of each plate was calculated using statically determined properties of the metal. If these energies differed, relative strengthening of different steels could be assumed. Predicted differences were from 5% to 39%. Average measured differences were 0% to 10%.

Thus the range of relative strengthening of mild steel over high yield steels was much less than would be predicted from laboratory experiments.

Thesis Supervisor: Frank A. McClintock
Title: Associate Professor of Mechanical Engineering

Cambridge 39, Massachusetts

21 May 1956

Professor Leicester F. Hamilton
Secretary of the Faculty
Massachusetts Institute of Technology
Cambridge 39, Massachusetts

Dear Sir:

In accordance with the requirements of the degree of Naval Engineer, we herewith submit a thesis entitled "The Relative Strengthening of Steels at the High Strain-Rates of Underwater Explosive Loading."

Respectfully,

James W. Lisanby
Lieutenant, USN

John E. Rasmussen
Lieutenant, USN

THE RELATIVE STRENGTHENING OF STEELS AT THE HIGH STRAIN-RATES OF UNDERWATER EXPLOSIVE LOADING

by

JAMES WALKER LISANBY, Lieutenant, U. S. Navy
B. S., U. S. Naval Academy, 1950

and

JOHN ELMER RASMUSSEN, Lieutenant, U. S. Navy
B. S., U. S. Naval Academy, 1947

SUBMITTED IN PARTIAL FULFILLMENT OF THE
REQUIREMENTS FOR THE DEGREE OF
NAVAL ENGINEER

at the
Massachusetts Institute of Technology
21 May 1956

Signature of Authors _____

_____

Certified by: _____
Thesis Supervisor

Accepted by: _____
Chairman, Departmental
Committee on Graduate
Students

ACKNOWLEDGEMENTS

The authors wish to acknowledge the valuable assistance and guidance of: Lieutenant Commander H. E. Henning, USN; Dr. A. H. Kiel and Dr. H. M. Schauer of the Underwater Explosions Research Division, Norfolk Naval Shipyard, Portsmouth, Virginia; and Professor F. A. McClintock, Massachusetts Institute of Technology.

ABSTRACT

THE RELATIVE STRENGTHENING OF STEELS AT THE HIGH STRAIN-RATES OF UNDERWATER EXPLOSIVE LOADING

by

James W. Lisanby and John E. Rasmussen

Submitted to the Department of Naval Architecture and Marine Engineering on 21 May 1956 in partial fulfillment of the requirements for the degree of Naval Engineer.

The purpose of this investigation was to investigate the relative strengthening of steels resulting from the high strain rates resulting from underwater explosions. Steel plates of equal size and shape, but of different composition, were subjected to the same explosive loading. The energy absorbed by the plastic deformation of each plate was calculated using statically determined properties of the metal. If these energies differed, relative strengthening of different steels could be assumed. Predicted differences were from 5% to 39%. Average measured differences were 0% to 10%.

Thus the range of relative strengthening of mild steel over high yield steels was much less than would be predicted from laboratory experiments.

Thesis Supervisor: Frank A. McClintock
Title: Associate Professor of Mechanical Engineering

TABLE OF CONTENTS

TABLE OF CONTENTS

(continued)

I. INTRODUCTION

A. Brief Description of Test

Ship's plating exposed to underwater explosions may be expected to have high strain-rates under certain conditions. The purpose of this investigation has been to find whether the increased stresses resulting from high rates of strain as found in the laboratory will be found in hot-rolled ship's plating with normal imperfections and residual stresses. It is also important to determine the different degree in which high strain-rates affect different steels.

For example, under certain laboratory conditions (2) an increase in flow stress for mild steel of 100% may be expected. The same conditions for a high yield strength steel could presumably result in an increase of 50% over the normal static stress. Thus a low carbon (mild) steel may have a strength of 100,000 psi under dynamic loading, and under the same conditions a high yield steel may have a strength of 150,000 psi.

This represents an absolute increase of resistance to plastic deformation by both steels. It also suggests a greater percentage strengthening for mild steels than for high yield strength steels.

This investigation consists of taking identical steel plates of various materials and exploding charges close enough to them to assure high rates of strain. The explosive energy going into the plates should be equal for explosions at the same distance.

Therefore, the energy measurable as plastic

distortion should be equal for equal charge distances. If this is not true using a normal static stress-strain curve for each material, then the high strain-rate must have alterred the relationship between stress and strain for the materials.

B. Theoretical Background

1. The Increase of Stress at High Strain Rates.

References one through five describe the effects of dynamic loading on the stress-strain relationship of steel. Of primary interest to this discussion are (1) the increase of upper and lower yield stress with increased rate of strain and (2) the difference of degree of this effect in different materials. Figure I shows the effect of strain rate on stress. The curve is reproduced from reference (1) and is a compilation of the work of several investigators.

The effect of this increase in dynamic stress may be seen by noting the consequent transformation of the stress-strain diagram as shown in Figure II from (3) and (24).

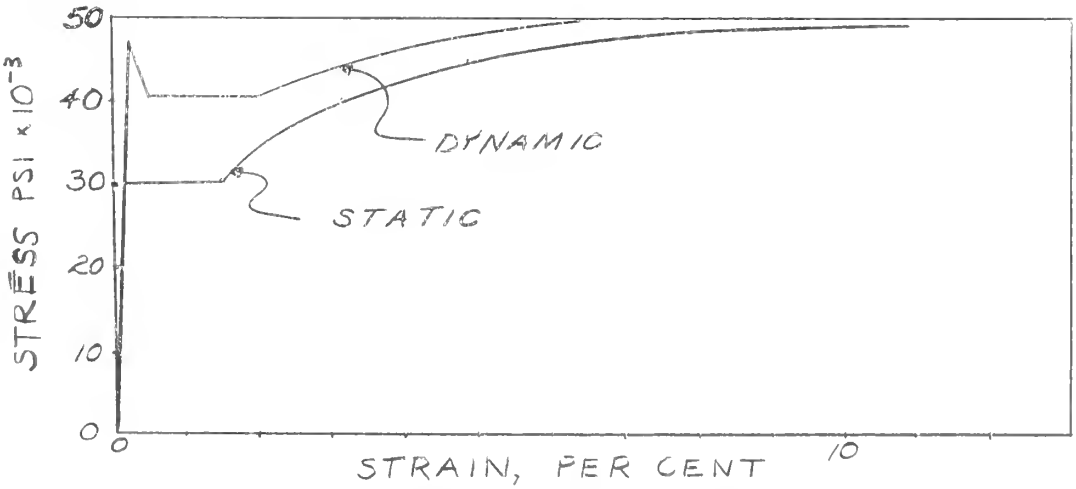

Figure II--Nominal Representation of Dynamic Stress-Strain Curve

FIGURE I

Dynamic-strengthening effect of strain rate in mild steel

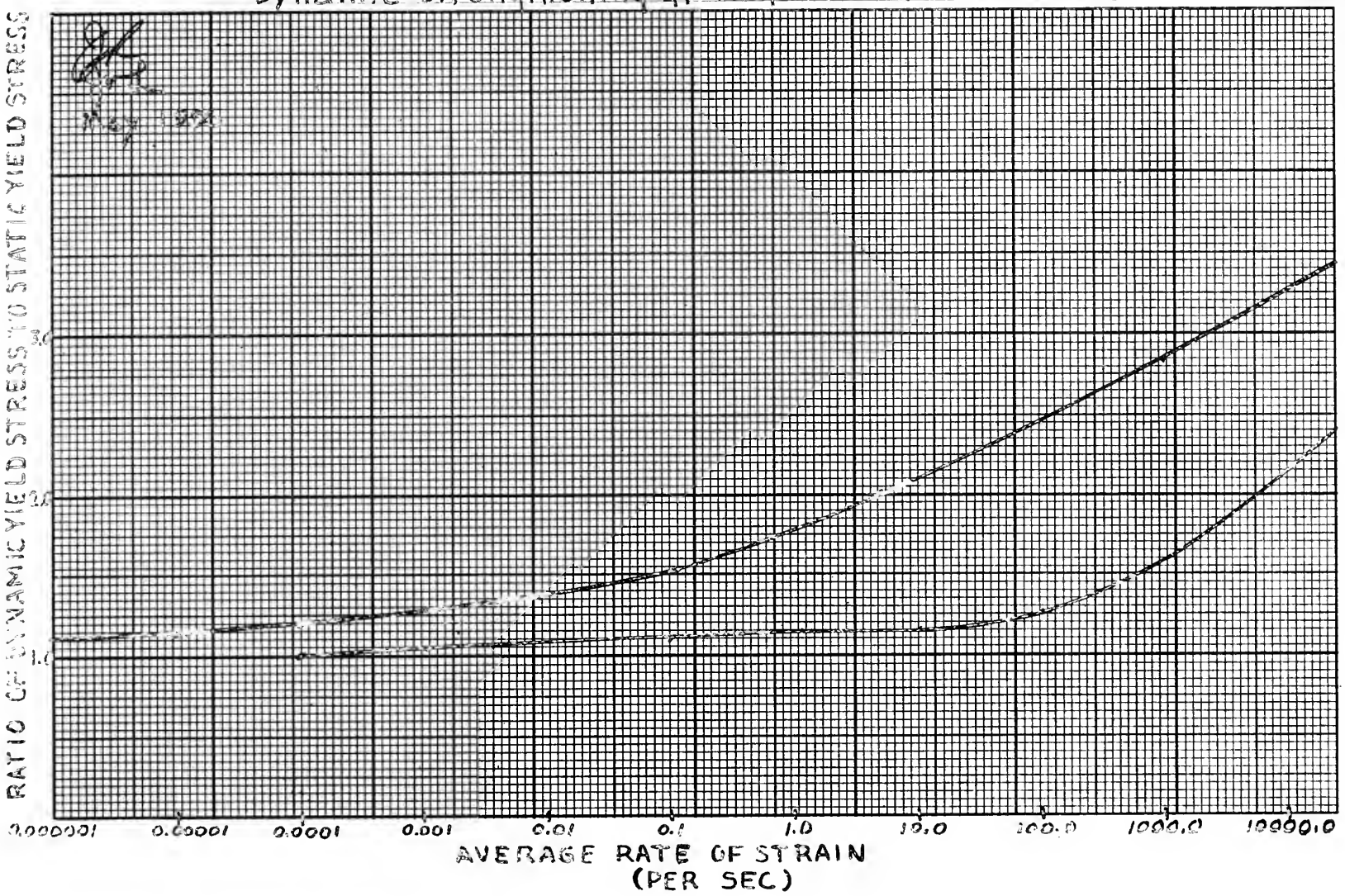

The second effect of interest is the difference of degree in which the stress is increased by strain rate for different materials. Since there is no such quantitative data available on the actual steel used in our tests, we have attempted to construct curves of probable values based on references (1) and (2). From these curves we may be justified in predicting the extent of the relative strengthening of mild steel over high yield steels.

Figure III gives the general characteristic of the ultimate and yield strength of steels as strain rate is increased. Table I shows quantitative values for the increase in ultimate strength of various steels. Table II gives the average values of static yield and ultimate strength for steels used in our tests.

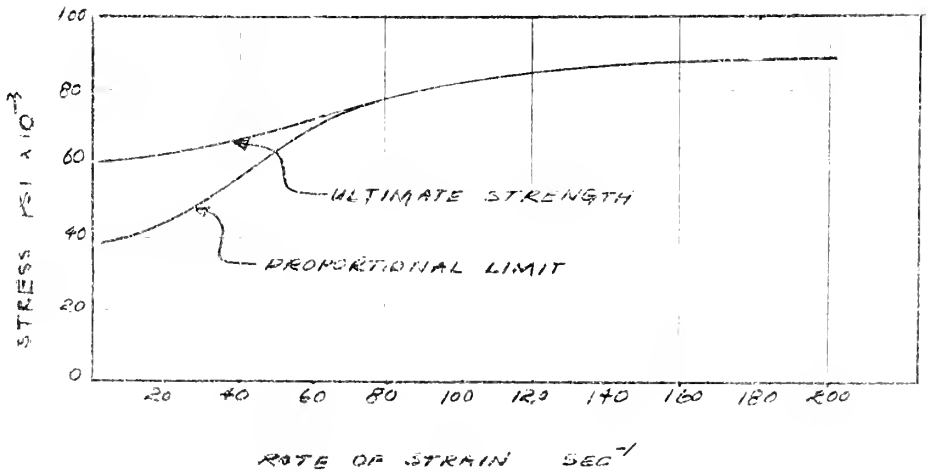

Figure III

From Clark (2) Showing Effect of Strain Rate on Proportional Limit and Ultimate Strength of a 0.22% Carbon Steel

TABLE I

From Clark (2) Increase of Ultimate

Strength at High Strain Rates

Material	Ultimate Strength		
	Static	Dynamic	% Increase
SAE 1015 Annealed	50,600	63,500	25.5
SAE 4140 Quench and Temper	134,250	151,000	12.4
Average of High Yield Steels	143,500	160,812	13.8

TABLE II

Average Strengths for Static Pull

Specimens of Materials Used in Tests

Material	Yield Strength	Ultimate Strength
Mild Steel	49,200	61,800
STS	103,900	116,700
HY-80	92,800	104,600
Average of All High Yield Steels	100,200	112,700

From these data Figure IV has been constructed. From Table II values of yield and ultimate strength were plotted on the "zero" strain rate ordinate. A value of ultimate strength at high strain rates was formed by increasing the static ultimate strength of each metal by the percent increase found for that metal in Table I. With these end point values, the curves were constructed to resemble Figure I.

If a specimen of each material is now pulled at a high strain rate, we should be able to predict the average increase in stress of the material during yielding from Figure IV. For a strain rate of twenty inches per inch per second

$$\frac{d\varepsilon}{dt} = 20 \text{ sec}^{-1}$$

We get yield stress values of

$$\sigma_{MS} = 56{,}600 \text{ psi}$$

$$\sigma_{MY} = 107{,}400 \text{ psi}$$

The percentage increase in stress is:

$$\Delta\sigma_{MS} = \frac{56{,}300 - 49200}{49{,}200} = 15.0\%$$

$$\Delta\sigma_{MY} = \frac{107{,}400 - 100{,}200}{100200} = 7.2\%$$

The values of percentage increase in yield stress for other strain rates are shown in Table III. This table shows that over a large range of strain rates mild steel shows a relative strengthening twice that expected for high yield strength steels.

FIGURE IV

Effect of strain rate on different steels

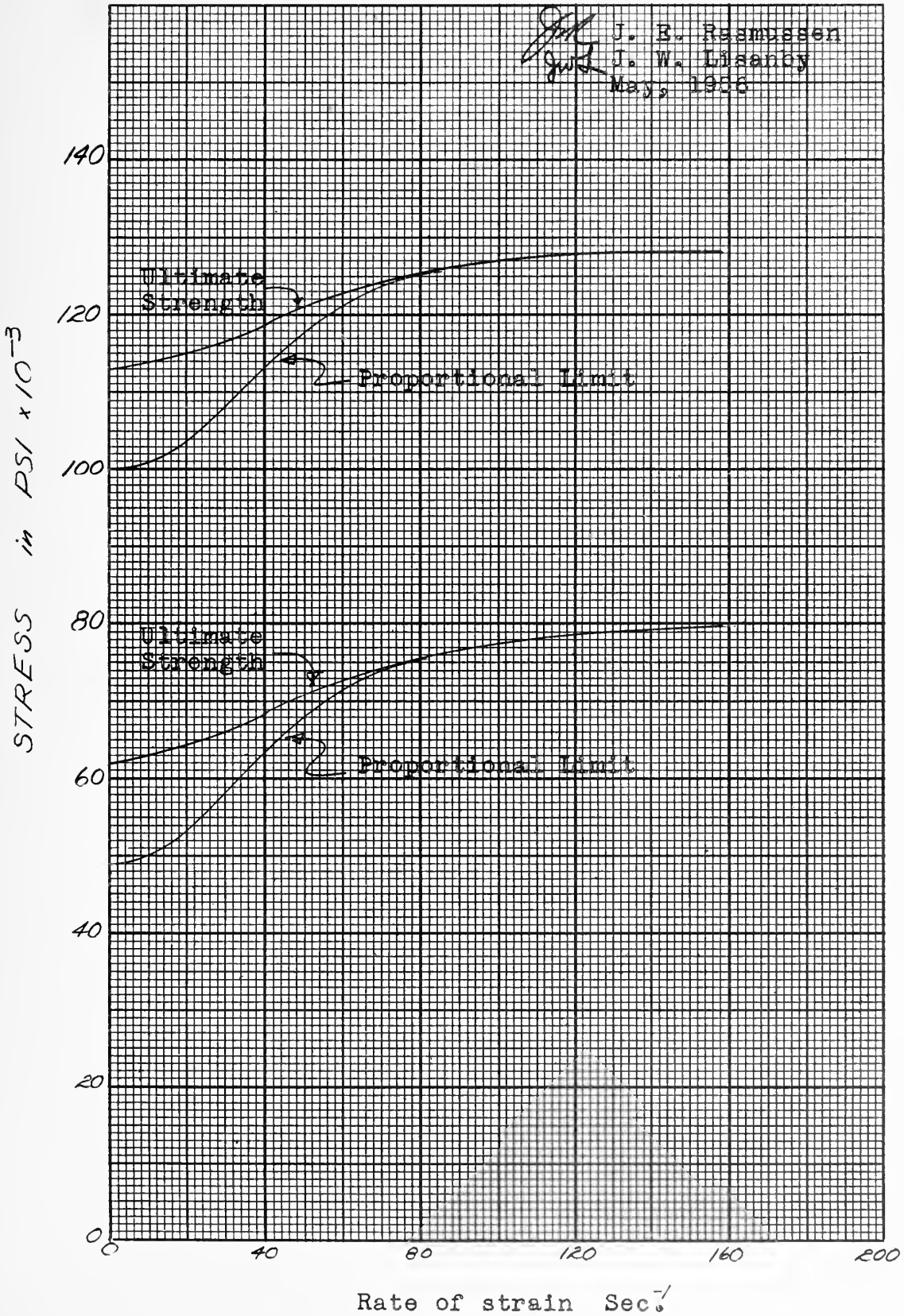

TABLE III

Comparison of Stress Increase in Mild Steel and High Yield Steels Under Dynamic Loading

Material	Strain Rate	Static Yield	Dynamic Yield	% Increase	Ratio
Mild Steel	20	49,200	56,600	15.0	2.08
High Yield	20	100,200	107,400	7.2	
MS	40	49,200	67,300	36.8	2.09
HY	40	100,200	117,800	17.6	
MS	60	49,200	73,200	47.3	2.05
HY	60	100,200	123,300	23.0	
MS	80	49,200	76,300	55.1	2.14
HY	80	100,200	126,000	25.7	

Therefore, to predict a stress increase in yield strength for a given strain rate we may enter Figure I for a factor of increase in mild steel. From Table III we would be justified in predicting a percentage increase for high yield steels of one half that for the mild steel. This differential stress increase the authors have termed the relative strengthening of mild steel.

2. Underwater Explosion Theory.

The ignition of a charge underwater gives rise to a pressure or shock wave in the water. If undisturbed, this pressure wave has a value at any distance which may be determined by the following equations (page 238 (6)).

$$P_m = (2.25)(10^4)\left(\frac{W^{1/3}}{R}\right)^{1.13} \qquad (1)$$

where: P_m = maximum pressure in lb/in^2

W = Weight of Pentolite in lb

R = Distance from explosion center in feet

The pressure at a given point builds up almost immediately to the maximum pressure, P_m, and then follows an exponential decay as shown in Figure V, where the decay time constant, θ, is (6)

$$\theta = 53.5W^{1/3}\left(\frac{W^{1/3}}{R}\right)^{1.13} \qquad (2)$$

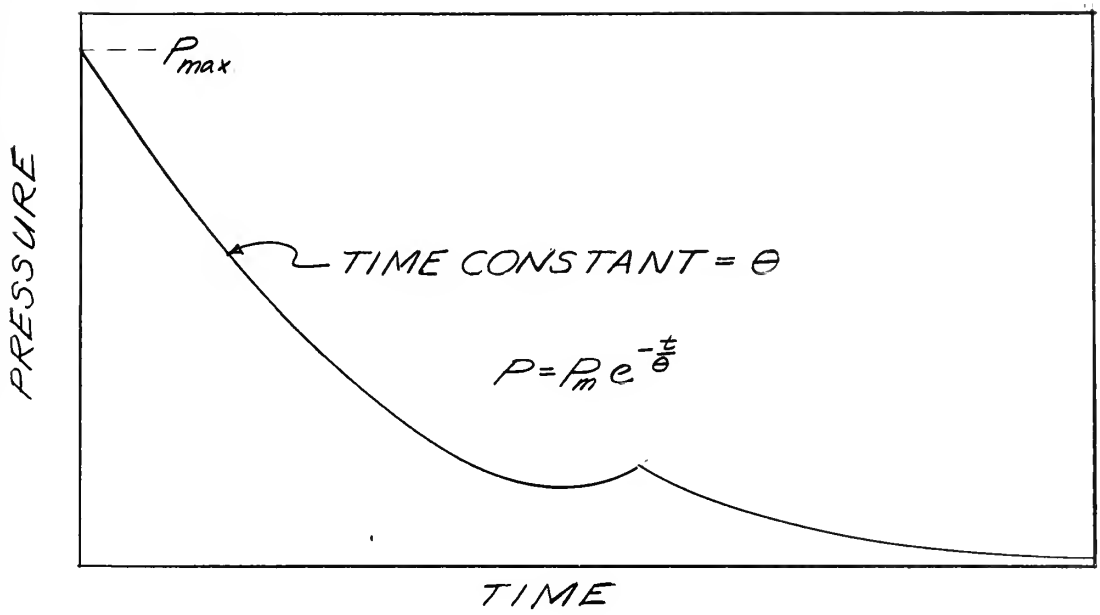

Figure V

Pressure at a Point Due to Shock Wave

From the physics of wave transmission, it can be shown that the pressure acting on an object of density much greater than that of water will be approximately twice the pressure in the water (6). This is due to the reflection of the wave from the denser medium.

Experimental observations of shock waves acting on air backed plates give characteristic curves as shown in Figure VI.

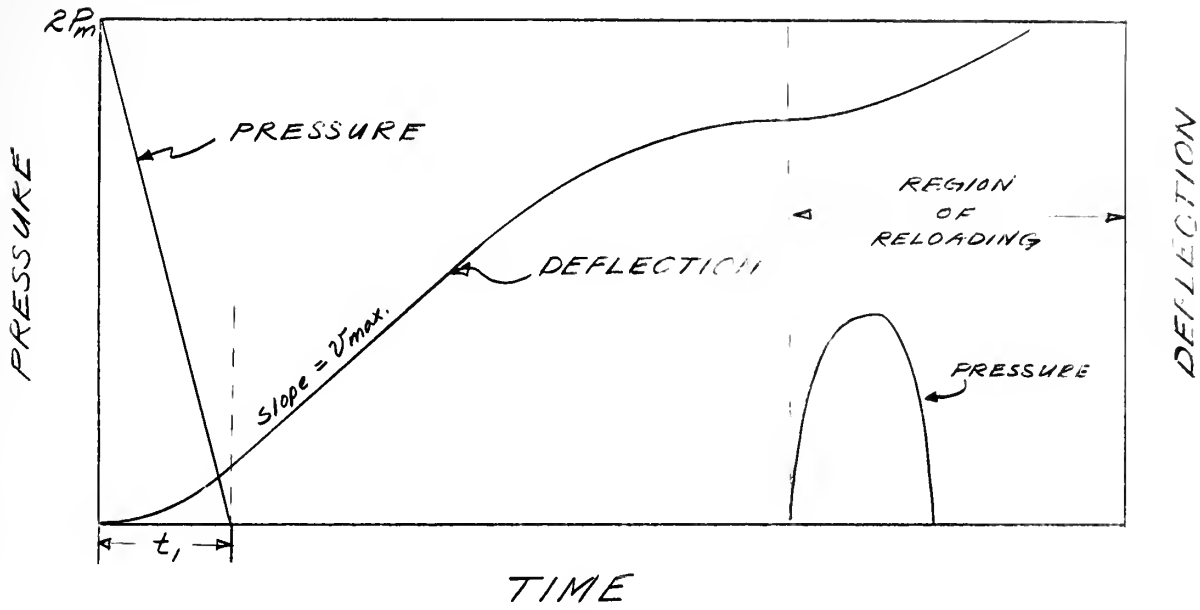

Figure VI

Characteristic Curves of Pressure and Deflection for An Air Backed Plate Exposed to Shock Wave

It can be seen that the pressure drops very quickly to zero as the plate accelerates. Since water cannot support tension, the plate breaks away from the water (cavitates) at the time of this zero pressure. The energy in the plate is then $\frac{1}{2}mv^2$. This energy will expend itself in plastic deformation of the plate at the same time the forces in the plate are decelerating it to zero velocity. The equation for plate motion up to the time of cavitation may be derived if certain assumptions are made. These simplifications are: (1) in the initial acceleration no restraints act on the plate, (2) the pressure of the air backing is constant, (3) the pressure is applied to the plate as a step of $2P_m$ with no build-up time, (4) the pressure is vented upward to the atmosphere before any reloading or second pressure pulse occurs, and (5) the plate moves as a

plane until cavitation. These conditions are all approximately fulfilled and are well within the accuracy of the overall tests.

Reference (6) equation 10.5 gives the equation for plate motion as:

$$m\frac{d^2Z}{dt^2} = 2P_m c^{-t/\theta} - \rho c \frac{dZ}{dt} \qquad (3)$$

where: m = Mass of the plate

Z = Deflection of the plate in a direction normal to its plane

ρ = Density of water = 64 lb/ft^3

c = Velocity of sound in water = 5000 ft/sec

Solution of this equation gives an expression for the velocity:

$$v = \frac{2P_m}{\rho c(1 - K)}\left(e^{-t/\theta} - e^{-t/K\theta}\right)$$

where $K = \dfrac{m}{\rho c \theta}$

The maximum velocity occurs at cavitation time, t_1:

$$V_{max} = \frac{2P_m}{\rho c} K^{\frac{K}{1-K}} \qquad (4)$$

$$t_1 = \frac{K\theta}{K - 1} \ln K$$

The one successful mechanical deflection gage (MDG) deflection history substantiated computed V_{max} values. Table IV gives values of maximum pressure, time constants, maximum velocity, cavitation time, and predicted explosive energies as functions of charge distance.

TABLE IV

Tabulation of Explosive Energy Values

R	P_m lb/in^2	θ x10^{-6} sec	v_{max} ft/sec	t_1 x10^{-6} sec	E ft-lb
4	11,200	136.7	210.5	61.1	15,300
5	8,720	145.4	166.6	62.2	9,590
6	7,100	153.2	137.7	63.9	6,550
7	5,970	160.0	117.2	64.8	4,760

The energy which eventually is calculated from plastic distortion due to the explosion should be the kinetic energy of the plate plus any water which continues on with the plate after cavitation.

$$E = \left(\tfrac{1}{2}mv^2\right)_{plate} + \left(\tfrac{1}{2}mv^2\right)_{water} \qquad (5)$$

Theory is inadequate to predict the amount of water or the thickness of water layer which may be carried with the plates after cavitation. However, the amount of water layer should be independent of the material of the plates. The comparison of computed plastic energy in the plates and the predicted explosive energy shows a probable water layer of about two-inch thickness.

From this derivation we see that the energy in a plate is a function of six variables: (1) plate mass, (2) density of water, (3) speed of sound in water, (4) water layer thickness, (5) charge weight, and (6) distance between plate and explosive. In our tests of $\frac{1}{4}$" steel plates, the first four parameters were effectively constant. Therefore, energy in a plate is a function only of its distance from the explosion and independent of the kind of steel used.

3. Materials Used.

Two different types of steel were used in this project. Mild steel is a U. S. Navy designation for a low carbon steel commonly used for ships' plating. STS and HY-80 are high yield strength, low alloy, special treated steels which are being used in some forms of ship construction. These two were chosen because of the predicted wide difference in their relative strengthening due to high strain rates and their availability in standard forms of $\frac{1}{4}$-inch ship plating.

Plates of corrosion resistant steel and HTS (heat treated steels) were also tested for comparison. There were not enough of these plates for suitable comparison. They will be plotted but not otherwise considered in the analysis.

The material analysis is given for all steels used in these tests in Appendix C, Summary of Data. This analysis includes the chemical composition by destructive tests, stress-strain characteristcs by tension tests and hardness tests. In addition, data is given in Appendix C of the true stress-strain measurements taken.

In all these tests it was found necessary to use stress-strain data for the immediate plate being considered. Comparable curves for the same material but different lots gave completely erroneous results.

4. Quantitative Expectation.

To predict the relative strengthening of mild steel over high yield strength steels, we must first determine an approximate magnitude of the strain rate found

in explosive loading. From Table IV we find V_{max} = 166.6 ft/sec for a five foot standoff. Assuming a linear deceleration, the time for the plate to come to rest is:

$$t_2 = \frac{2Z_{avg}}{V_{max}} \qquad (7)$$

All strains were completed before this time. Then a bounding or minimum value of average strain rate would be:

$$\left(\frac{d\varepsilon}{dt}\right)_{avg} \geq \frac{\varepsilon_{avg}}{t_2} = \frac{\varepsilon_{avg} V_{max}}{2Z_{average}}$$

For a typical plate at 5 foot standoff these values are:

Z_{avg} (at r = 5") = 1.82 inches

$\varepsilon_{avg} \approx 0.0582$

$$\left(\frac{d\varepsilon}{dt}\right)_{avg} \geq \frac{(0.0582)(166.6)(12)}{(2)(1.82)} = 32$$

DY-8 is a high yield steel at 5 feet. Z = 1.12, ε_{avg} = 0.0217.

$$\left(\frac{d\varepsilon}{dt}\right)_{avg} \geq \frac{(0.0217)(166.6)(12)}{(2)(1.12)} = 19.4$$

These values of strain rate are of the same order of magnitude and should be sufficient to enter Figure I to find the increase in stress we should expect for mild steel. For a strain rate of thirty, we get predicted values of dynamic to static yield stress ratios of:

$$\left(\sigma/\sigma_y\right)_{max} \cong 2.25$$

$$\left(\sigma/\sigma_y\right)_{avg} \cong 1.70 \qquad \frac{d\varepsilon}{dt} \approx 30 \text{ sec}^{-1}$$

$$\left(\sigma/\sigma_y\right)_{min} \cong 1.20$$

At a strain rate of 15 sec^{-1} the following predictions would be made from Figure I:

$$\left(\sigma/\sigma_y\right)_{max} \simeq 2.2$$
$$\left(\sigma/\sigma_y\right)_{mean} \simeq 1.65$$
$$\left(\sigma/\sigma_y\right)_{min} \simeq 1.15$$

It can be seen that within this range of strain rates, the difference in predicted ratios is such that even greater strengthening than that predicted in Table III should be observed in our tests.

If we assume all the original kinetic energy of the plate goes into the plastic distortion of the plate, we can then calculate this energy as a function of plastic strain from a static stress-strain curve for the material. If no dynamic increases in flow stress occur, this method for computing energy by reliance on the static stress-strain characteristic should be valid. Since the kinetic energy of the plate is a function only of charge distance, the computed energies of all plates shot at a given distance should be equal regardless of material.

If dynamic strengthening of mild steel and high yield steels exists in our plates, then calculation of energy by use of static stress-strain curves will be in error. Since energy is an approximately direct function of yield stress, we should be able to find the actual energy by multiplying the calculated energy by the expected ratio of dynamic stress increase.

$$E_{actual} = \frac{\sigma \text{ dynamic}}{\sigma \text{ yield}} \times E \text{ calculated} \qquad (9)$$

All actual energies at one standoff must be equal regardless of material or dynamic properties. Therefore, we may find a

comparison of dynamic strengthening in two steels as follows:

$$E_{actual} = \frac{(\sigma_d)}{(\sigma_y)_{HY}} \times E_{HY} = \frac{(\sigma_d)}{(\sigma_y)_{MS}} \times E_{MS} \qquad (10)$$

$$\frac{\left(\frac{\sigma_d}{\sigma_y}\right)_{MS}}{\left(\frac{\sigma_d}{\sigma_y}\right)_{HY}} = \left(\frac{E_{HY}}{E_{MS}}\right)_{computed} \qquad (11)$$

Our average value of $\frac{\sigma_d}{\sigma_y}$ as chosen from Figure I may be conservatively estimated as 1.50 for mild steel. This is an increase of 50% over the static yield strength. From Table III we are justified in assuming that a comparable increase in $\frac{\sigma_d}{\sigma_y}$ for the high yield steels would be 25% or

$$\left(\frac{\sigma_d}{\sigma_y}\right)_{HY} = 1.25$$

Therefore, we should predict on the basis of laboratory investigations that the calculated energy ratios of high yield steels to mild steels will be:

$$\left(\frac{E_{HY}}{E_{MS}}\right)_{computed} = \frac{1.50}{1.25} = 1.2$$

Or that their percentage differences would be:

$$\frac{E_{HY} - E_{MS}}{E_{MS}} = \frac{1.50 - 1.25}{1.25} = \underline{\underline{20\%}} \qquad (12)$$

A lowest possible predicted value may be estimated from the lower curve of Figure I.

$$\left(\frac{\sigma}{\sigma_y}\right)_{MS} = 1.20$$

Values from Figure I are taken for increase in lower yield point. To be more conservative let us assume that the average increase over the entire range of strain is only

one half this value. Then:

$$\left(\frac{\sigma}{\sigma_y}\right)_{MS} = 1.10$$

A comparable value for high yield steels may be estimated to again give one half this increase:

$$\left(\frac{\sigma}{\sigma_y}\right)_{HY} = 1.05$$

Then as in equation (11)

$$\left(\frac{E_{HY}}{E_{MS}}\right) = \frac{\left(\sigma/\sigma_y\right)_{MS}}{\left(\sigma/\sigma_y\right)_{HY}} = \frac{1.10}{1.05} = 1.05 \qquad (13)$$

This says that a most conservative probable value would show a relative strengthening of mild steel over high yield steels of five per cent.

It must be borne in mind that these predicted values are all based on laboratory tests performed on samples with no imperfections and lacking the residual stresses of normal structures. Our tests are an attempt to determine the validity of these predictions in normal built-up structures.

C. Energy Calculations: General

Various methods were proposed and tried for computation of the energy in the plates to allow comparison of test results with the predictions of equations (12) and (13).

The first method tried was an attempt to compare energies by the ratio of their lower yield stress and the square of the center deflection.

$$\frac{E_{HY}}{E_{MS}} = \frac{(\sigma_y Z_c^2)_{HY}}{(\sigma_y Z_c^2)_{MS}} \qquad (14)$$

This method is an approximation to a more accurate procedure of using an area strain.

$$_A = \frac{\Delta A}{A}$$

Since the large deflections found in our tests tended to invalidate the deflection squared comparison, we determined to calculate an accurate value of ΔA and use it in energy comparisons.

$$\frac{E_{HY}}{E_{MS}} = \frac{(\sigma_y \ \Delta A)_{HY}}{(\sigma_y \ \Delta A)_{MS}} \qquad (15)$$

The results of these methods are covered briefly in Appendix B-2.

The theoretical uncertainty of the above results gave rise to attempts to calculate the energy by more orthodox methods. The plate was considered as a three dimensional body where strains were measured in the directions of radius, circumference, and thickness.

ε_r = Radial strain

ε_θ = Circumferential strain

ε_h = Thickness strain

Since the predominant part of the energy is in the membrane stretch of the plates, it can be seen that one way of computing energy would be:

$$\frac{E}{V} = \int \sigma_r \, d\varepsilon_r + \int \sigma_\theta \, d\varepsilon_\theta \qquad (16)$$

where the integrals are determined by integrating over the appropriate stress strain curve to the measured value of

strain. This method is covered in Appendix B-3 .

Another method is suggested by the fact that the stretching stress in the radial and circumferential directions causes thinning in the thickness direction. An appropriate compressive stress in the thickness direction would result in an approximately comparable set of strains in the radial and circumferential directions. Therefore, energy may be considered a function only of this thickness strain.

$$\frac{E}{V} = \int \sigma_h \, d\varepsilon_h \qquad (17)$$

A theoretically more accurate method is that represented by the effective stress-strain relationship (23) which takes into account the effective plastic "poisson's ratio" and two dimensional work hardening. This method is discussed in Appendix B-1 and used to verify the validity of approximate methods used.

If the plate travels as a plane while distortion takes the form of a plastic hinge traveling from the periphery inward, energy will be expended in this bending and unbending of the hinge. Since little is known of this process, it is not considered in our analysis. It is considered that any such action will appear as distortion or plastic strain and be included in the computed energy.

II. PROCEDURE

A. Apparatus

Figure VII shows the large 32" diameter steel drum with outrigger. The outrigger carries a ten pound charge of pentolite centered at the standoff distance, R, from the center of the plate. All explosions were conducted with two feet of water over the center of the drum and charge.

Figure VIII shows a plate welded at its outer edge to the backing drum. Figure IX gives a detailed schematic view of the plate and drum. The backing plate is secured by 20 nuts and tested for tightness before each shot. Several stuffing tubes are provided for instrumentation of the plates.

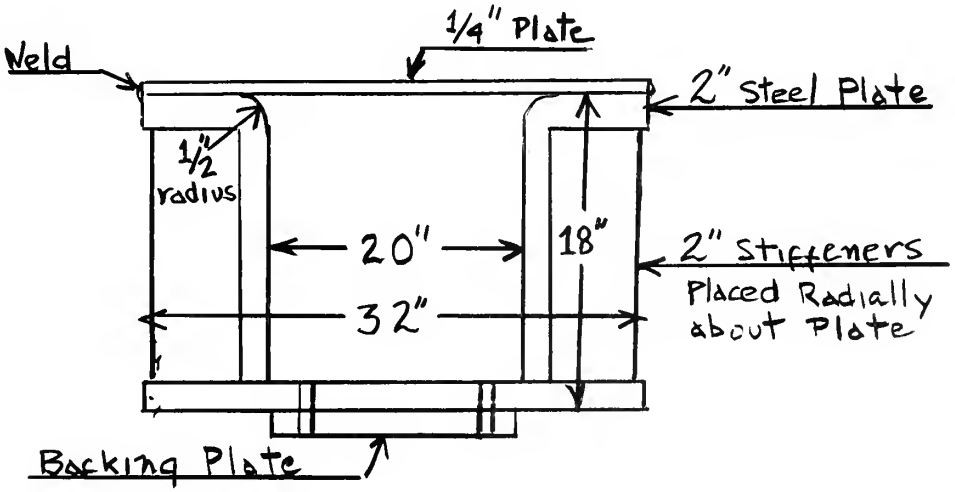

Figure IX. Schematic of Drum and Plate

B. Measurements

Deflection readings, Z, were taken on all plates before and after explosions as shown in Figure X. Readings are accurate to the 0.01 inch.

FIGURE VIII
View of Plate as
Welded to Drum

J. E. Rasmussen
J. W. Lisanby
May, 1956

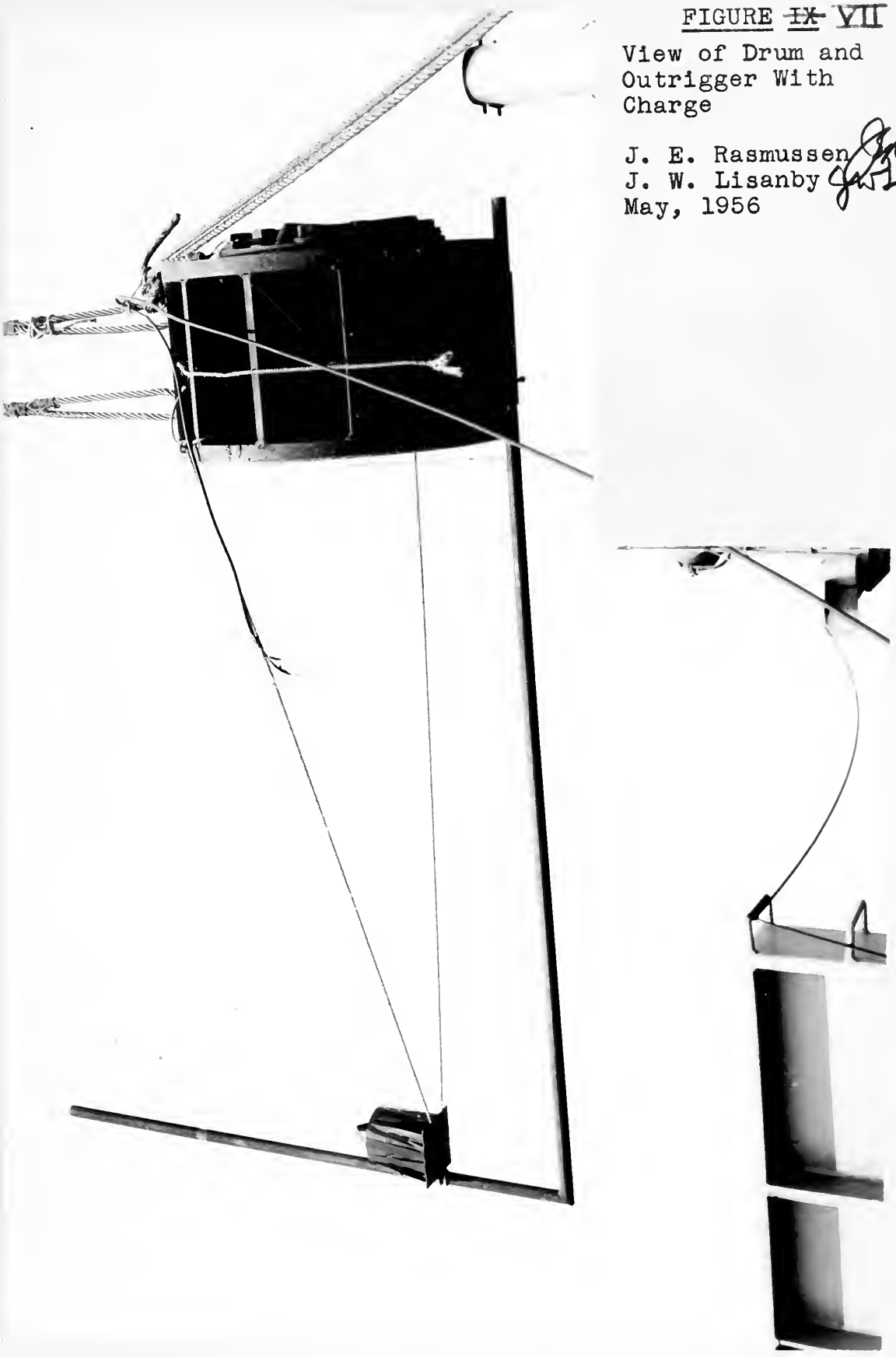

FIGURE ~~IX~~ VII

View of Drum and Outrigger With Charge

J. E. Rasmussen
J. W. Lisanby
May, 1956

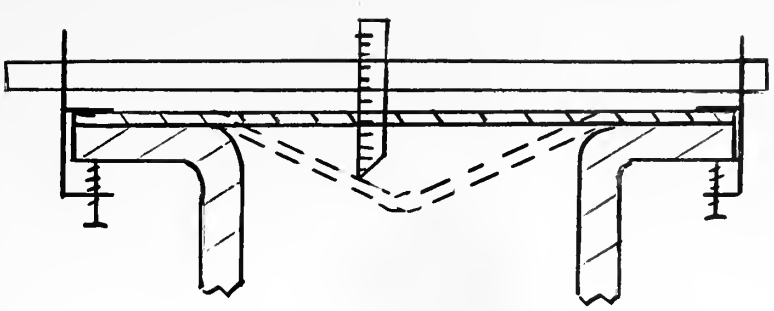

Figure X. Illustration of Deflection Readings

On several plates (DY 1-3, 7-9, 27-34) punch marks were placed along two plate diameters at radii, 0, 1, 3, 5, 7, 9, 11. These punch marks were made with a two inch jig. Readings before and after explosion were made with an accuracy of 0.0001 inch. These were used to determine radial strains. Readings over shoulder and center were made with flexible steel tape: accuracy 0.01 inch.

Movement of punch marks away from the center was recorded for the purpose of determining circumferential strains from the consideration that $\bar{\varepsilon} = \frac{\Delta r}{r}$. These readings were accurate only to 0.05 inch.

After the explosion, most of the plates were cut along one diameter (see Figure XI). Thickness readings were taken along this diameter by micrometer of accuracy 0.0005 inch. Paint and scale were removed prior to readings. Readings were taken at original radii by use of punch marks as reference or by laying out approximate radius from comparison with previous plates with punch marks.

Arithmetic averages of original data are tabulated in Appendix C. Original readings of two plates are given in Appendix F to show degree of anisotropy.

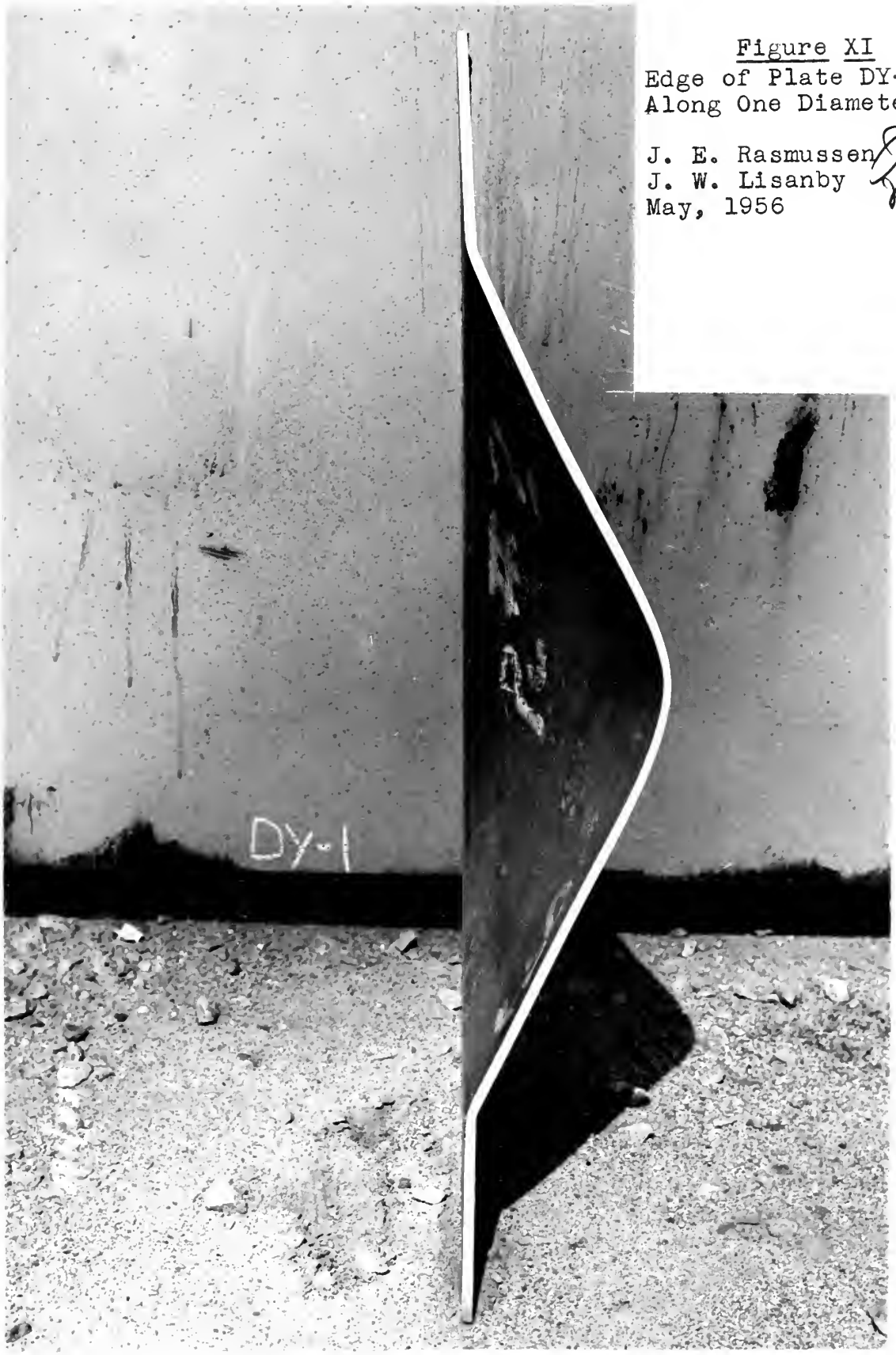

Figure XI
Edge of Plate DY-1 Cut
Along One Diameter

J. E. Rasmussen
J. W. Lisanby
May, 1956

Dynamic measurements were made during various tests with strain gages mounted on the inside of plates and with mechanical deflection gages. The results were not completely successful except to confirm our value of initial plate velocity. The major problem encountered was to get strain gages which would stick to the plate during the violence of explosion and measure the large strains. The deflection gages suffered from the high decelerations.

To obtain dependable stress-strain curves for calculations of energy, samples from each plate were taken and machined to give an accurate circular cross section. As the specimen was pulled, continual measurements of diameter were taken to give an accurate value of stress strain in the region of necking down. Diameter readings were taken with a conical micrometer to an accuracy of 0.0005 inches. Original stress-strain data is given under original data in Appendix C.

C. Stress-Strain Curves

Stress-strain curves were plotted using the data given in Appendix C. Engineering stress and strain were used for ease of calculation.

Where $\overline{\sigma} = \frac{F}{A_o}$

$$\overline{\varepsilon} = \frac{l - l_o}{l_o} = \frac{A_o - A}{A} \qquad (18)$$

After the curves were plotted an integraph was used to trace the value of energy per unit volume on the graph as a function of strain. This allows finding the energy per unit volume directly from the graph by entering

with an appropriate value of strain. The decision as to the type of strain to be used for entering the graph will be discussed below.

D. Energy Calculations

To determine the existence of the dynamic stress differential predicted in equation (12), it is necessary to devise a method for finding the energy in the plate.

Elastic energy may be shown to be small:

$$E_e = V\int \sigma \, d\varepsilon$$

where $\sigma = Y\varepsilon = \sigma_{yield}$

$$E_e = V\int \sigma \frac{d\sigma}{Y} = \frac{V\sigma^2}{2Y} \qquad (19)$$

Comparison of DY-2 for mild steel and DY-8 for a high yield steel at equal standoffs gives the following elastic energies.

$(E_e)_{MS}$ = 392 foot pounds

$(E_e)_{HY}$ = 1440 " "

The average total energy at this standoff is 21,360 ft-lbs. Therefore, at most, the elastic energy represents only 7% of the total energy.

The actual measure of energy was done by integrating over the stress-strain curve. Since the stress-strain curve was plotted as a rigid-plastic curve, the elastic energy was largely included in the integration. This can be seen in Figure XII. This approximate inclusion of elastic energy is warranted due to the small percentage of total energy represented by the elastic energy.

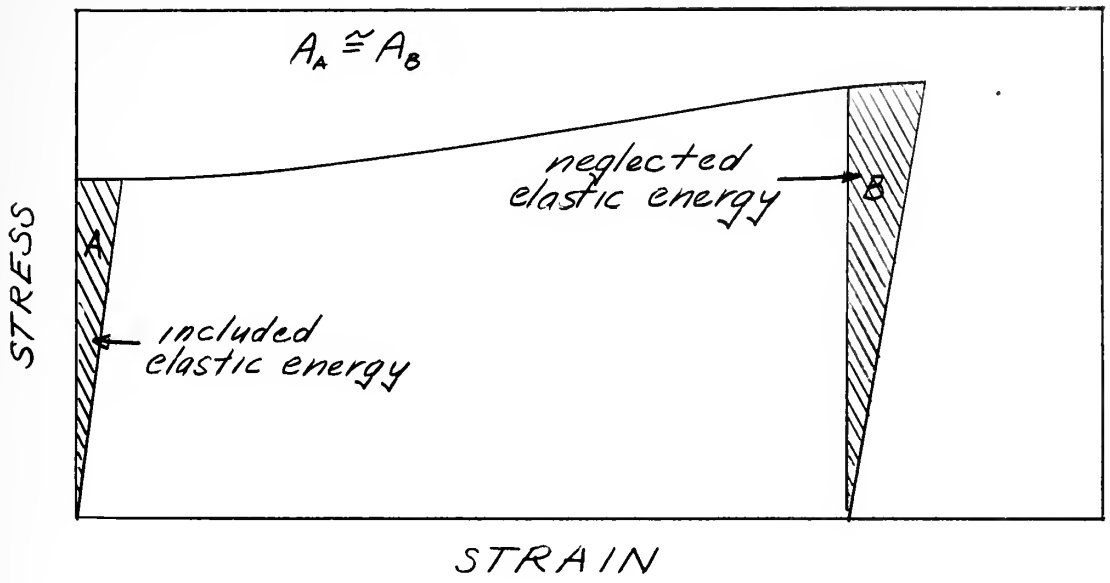

Figure XII. Approximate Accounting for Elastic Energy

Several methods have been employed to determine the plastic energy in the plates. We have treated separately the energy due to bending and that due to membrane action. The bending energy is of secondary importance and hence is treated in an approximate manner. This approximate method requires only that the Yield stress be considered constant over the entire plate and that the shape of the distorted plate be considered conical.

Bending Energy: If we consider only bending around the edge of the air backed portion of the plate, the plastic strains are large enough to treat the stress as being independent of distance from the neutral axis. Figure XIII-a shows such a distribution.

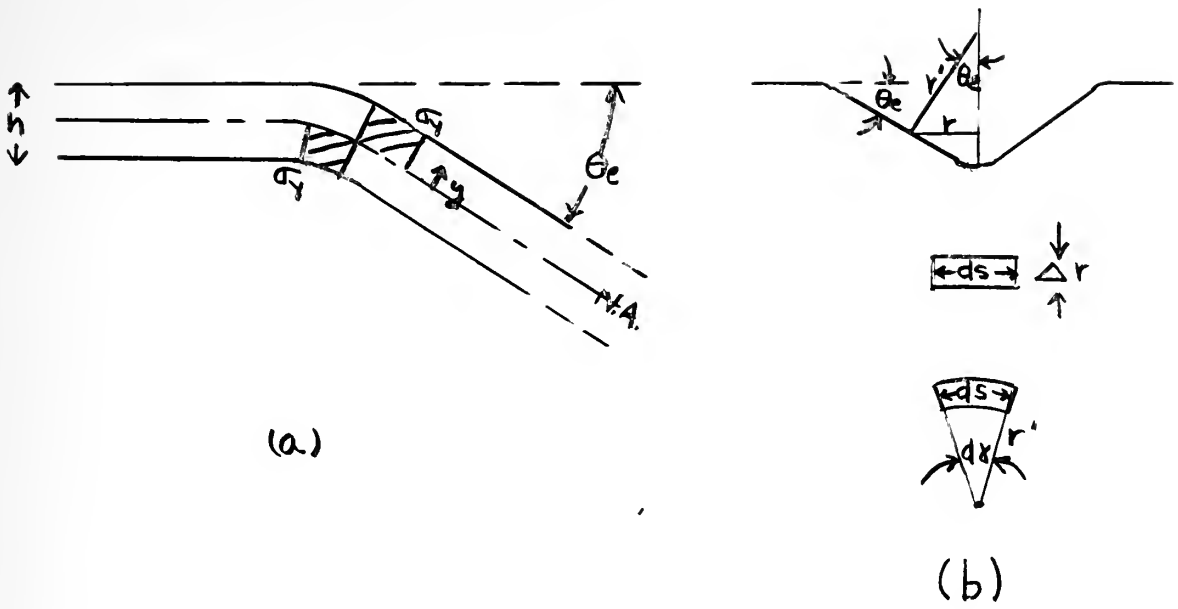

Figure XIII. Methods for Determining Bending Energy

The moment, M_o

$$M_o = 2\int_0^{h/2} \sigma_y y dy = \frac{\sigma_y h^2}{4} \tag{20}$$

$$E = M_o \theta_e \pi D = \frac{\pi D h^2}{4} \sigma_y \theta_e \tag{21}$$

where E_b is the energy over the entire circumference.

In the rest of the plate, bending exists in the circumferential direction. If we neglect the effect of tensile stress in the plate, we can derive the following conservative relationship from Figure XIII-b. For any one annular ring of width Δr, at radius r, the energy will be:

$$\Delta E = \Delta r \int M d\gamma = h \Delta r \int M \frac{ds}{r'}$$

$$= \Delta r \int M ds \frac{\sin \theta_e}{r} \tag{22}$$

If we let M_o be the ideal plastic moment and constant over the entire range of strain, then we may integrate around the annular ring.

$$\Delta E = \frac{\Delta r\, M_o}{} 2\pi \sin \theta_e$$

θ is small and constant over the plate. Integrating with respect to r,

$$E = \int_0^{D/2} M_o\, 2\pi\theta_e dr = 2\pi M_o \theta \frac{D}{2}$$

$$E = \frac{\pi D h^2}{4} \sigma_y \theta_e \tag{23}$$

Thus the total bending energy is twice the bending energy at the edge.

$$E_b = \frac{\pi D h^2}{2} \sigma_y \theta_e \tag{24}$$

Values of total bending energy are tabulated in Table V.

TABLE V

CALCULATION OF BENDING ENERGY

DY	Σ_h edge	$\bar{\sigma}$ edge	θ°	θ rad	E_b
1	.05	51,000	24.7°	.431	3600
2	.033	46,400	19°	.332	1520
3	.014	43,200	15.3°	.267	1888
4	----	------	-----	----	----
5	.012	66,000	17.4°	.304	2694
6	.027	66,500	23°	.401	3584
7	.016	112,600	15°	.262	4820
8	.001	111,800	11°	.192	3510
9	0	111,800	8.5°	.148	2706
10	.024	45,500	20.5°	.358	2662
11	.041	45,500	26°	.454	3380
12	.014	45,500	16.7°	.292	2170
13	.012	93,000	17.2°	.300	4560
14	.0085	92,000	12.5°	.218	3280
15	.001	90,500	9.5°	.166	2618
16	.014	47,000	23.5°	.410	3050
17	.02	47,000	19°	.332	2554
18	.01	47,000	12.7°	.222	1706
20	.014	99,000	20.0°	.349	5840
21	.015	99,000	12°	.209	3380
22	.018	51,000	18.1°	.316	2640
25	0	111,800	8.1°	.141	2706
27	.002	111,000	7°	.122	2220
30	.025	45,500	13°	.227	1700
31	.019	45,000	19°	.331	2440
32	.0026	45,000	15°	.261	1920
33	.015	45,000	15½°	.270	1990
34	.160	61,000	25°	.436	4370

The membrane energy has been computed in various ways in this investigation to find a suitable compromise between theoretical accuracy and available data. Several of these methods are covered in Details of Procedure, Appendix B. The method used for the final calculation of results was chosen because adequate data was available to compute the energy of most plates, and it is theoretically acceptable. According to this method:

$$\Delta E = \Delta V \int \sigma_h d\epsilon_h \qquad (25)$$

where: ΔV = an increment of plate volume

$\epsilon_h = \ln \frac{h}{h_o}$ = true strain

σ_h = true stress from static stress strain curve

Thickness strains at various points of the plate were calculated and the energy was then integrated over the stress-strain curve and over the entire plate area.

This method is exact (13) only when the stresses in the other two axial directions are equal. Figure XIV shows strains in each of three axes: radial, circumferential, and thickness for a sample plate. It can be seen that the requirement $\epsilon_r = \epsilon_\theta$ is met to a reasonable degree where energy comparisons are desired instead of absolute energy values. Theoretically correct energies have been computed for several plates using effective strains (23) as arguments for entering the stress-strain curves. These calculations for DY-1, 2, 3 are shown in Details of Procedure, Appendix B. Figure B-1 shows the close agreement between

FIGURE XIV

Average Strains , DY-1

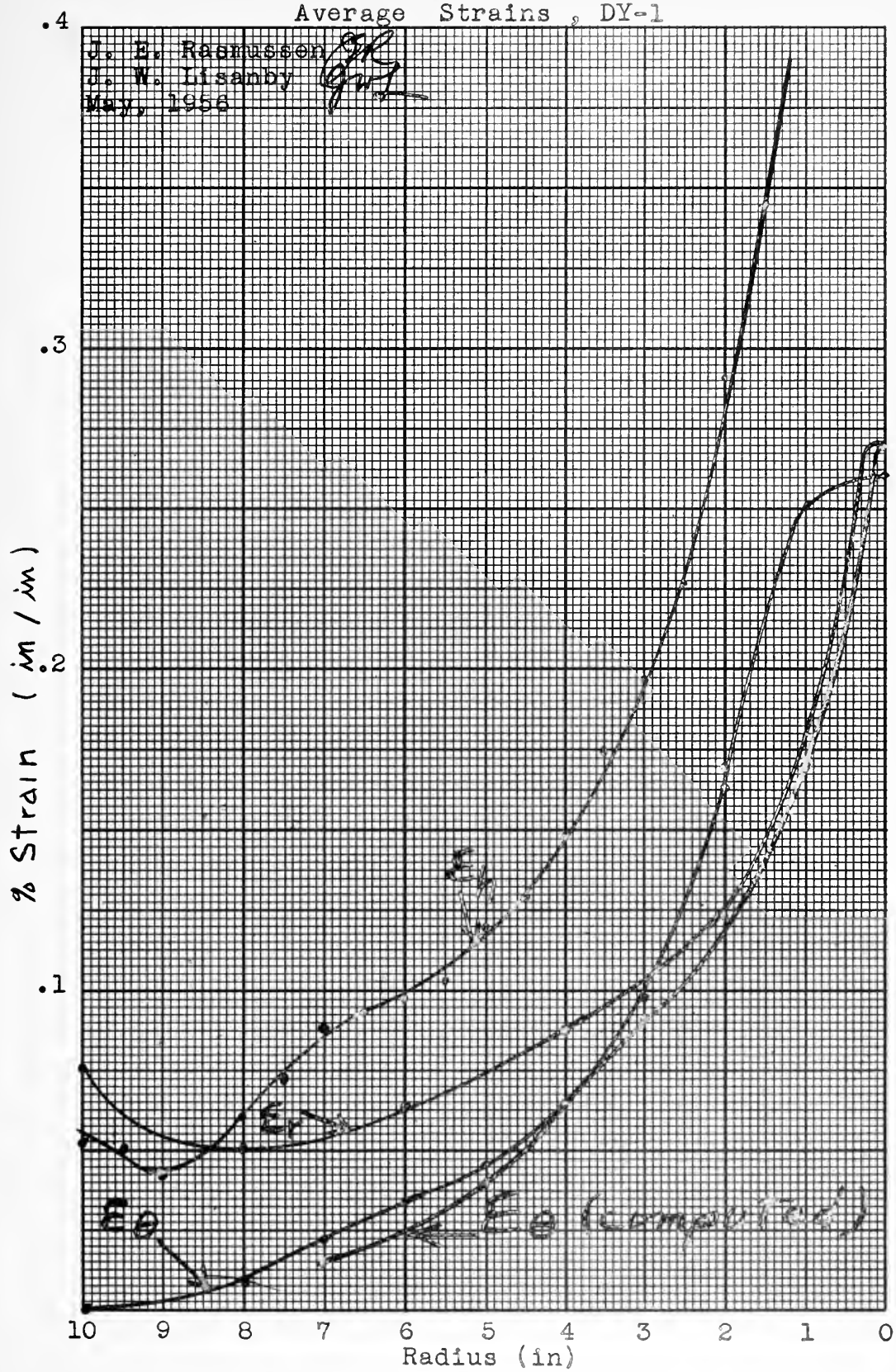

these theoretically correct energy values and those computed by thickness strains only.

The thickness strain, ε_h, is an "effective compressive" strain since one might expect compression of the plate to give approximately the same biaxial strains which resulted from the biaxial stresses in the plate. However, if the energy is calculated using this "compressive" strain, it may be necessary to use true stress-strain curves to get correlation between the tensile specimens on which the curves are based and the compressive strains which are used for arguments (Reference 13, page 28). It is much easier to plot curves of engineering stress and strain. Therefore, an equivalent argument may be determined which will allow entering the engineering stress-strain curves to get the energy based on true strain.

Equation (26) shows that energy is independent of the type of stress-strain used.

$$E = \int F dx = \int \frac{F}{A_o} A_o \frac{dx}{x_o} x_o = A_o x_o \int \bar{\sigma}\, d\bar{\varepsilon} \qquad (26)$$

$$= \int \frac{F}{A} A \frac{dx}{x} x = Ax \int \sigma\, d\varepsilon$$

Therefore:

$$\int \sigma\, d\varepsilon = \int \bar{\sigma}\, d\bar{\varepsilon}$$

To determine the equivalence of true strain and engineering strain: From (13)

$$\varepsilon_{\text{compressive}} = -\varepsilon_{\text{tensile}} = -\ln \frac{l}{l_o} \qquad (27)$$

Our curves as an engineering strain:

$$\bar{\varepsilon} = \frac{l - l_o}{l_o} = \frac{l}{l_o} - 1 = e^{\varepsilon_r} - 1$$

Then $\frac{l - l_o}{l_o} = e^{-\varepsilon_c} - 1 = e^{-\ln\frac{h}{h_o}} - 1 = \frac{h_o}{h} - 1$

$$\frac{l - l_o}{l_o} = \frac{h_o - h}{h} \tag{28}$$

Therefore, enter stress-strain curves with

$$\varepsilon = \frac{h_o - h}{h} \tag{29}$$

to find energy per unit volume.

The strain varies greatly from the center of the plate to the periphery with highest strains at the center. To account for this increased stress due to work hardening, the plate was divided into annular rings of $\Delta r = \frac{1}{2}$ inch. The strain was taken from a faired plot of strains for the mean radius of each ring. With this strain a value of energy per unit volume was taken from the stress-strain curve.

$$\Delta E = \Delta V_r \int \sigma \, d\varepsilon$$

The energy of all rings was then summed to find the total plate energy. A sample calculation is shown in tabular form in Sample Calculations, Appendix D.

III. RESULTS

Results are presented in the form of a calculated value of the energy absorbed by each experimental plate using the method of energy calculation proposed by the authors that $E = V\int \sigma_h d\varepsilon_h + E_b$ where the symbols are again defined as:

E = Energy of plastic deformation in foot pounds

V = Total volume of the metal so deformed

σ_h = Static yield stress of the metal

$\Delta\varepsilon_h$ = Thickness strain $\frac{h_o - h}{h}$

E_b = Bending energy

Table VI presents the tabulation of this information specifying test number and material of each plate for identification. Figure XV presents the information graphically as a plot of energy absorbed by each plate versus standoff distance between plate and explosive. Used in this manner standoff distance is a measure of input energy.

TABLE VI

TABULATION OF CALCULATED VALUES FOR ENERGY ABSORBED

Plate No.	Stand-off (ft)	Material	Energy Absorbed (Foot-Pounds)
DY-1	4	Mild Steel	37,600
DY-2	5	" "	21,410
DY-3	6	" "	11,890
DY-7	4	Special Treatment Steel	35,450
DY-8	5	" " "	20,200
DY-9	6	" " "	17,800
DY-10	5	Corrosion Resistant Steel	21,700
DY-11	4	" " "	44,400
DY-12	6	" " "	13,660
DY-13	4	HY-80	35,700
DY-14	5	"	22,500
DY-15	6	"	12,270
DY-16	4	Mild Steel	37,600
DY-17	5	" "	18,230
DY-18	7	" "	9,850
DY-20	3.5	Special Treatment Steel	58,100
DY-21	5	" " "	24,180
DY-25	6	" " "	13,500
DY-27	7	" " "	7,350
DY-30	7	Mild Steel	8,170
DY-31	5	" "	21,300
DY-32	7	" "	7,800
DY-33	6	" "	13,060
DY-34	4	" "	34,800

FIGURE XV

Energy Absorbed By Plastic Deformation VS Standoff

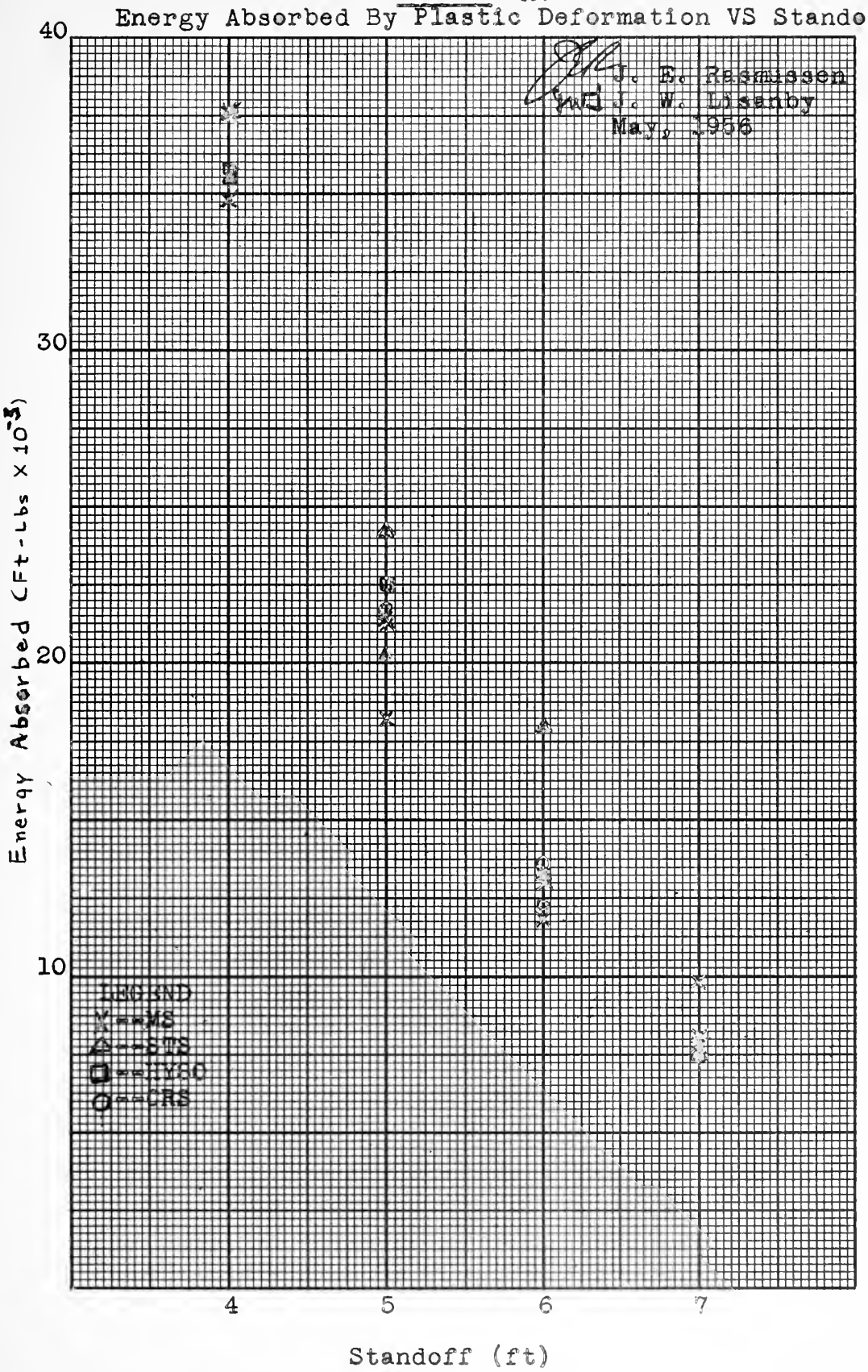

IV. DISCUSSION OF RESULTS

The discussion of the results obtained from the calculated values of energy absorbed in each of the experimental tests rests on one important concept. This consideration is that with no increased dynamic strengthening of the mild steel over the high yield steels the values of the energy absorbed as calculated for the two groups should be equal. If mild steel should exhibit this relative increased strengthening effect, the value of the energy absorbed by mild steel as calculated from the static stress-strain curves, assuming no dynamic effect, will be lower than that calculated for the low alloy, high yield steels. Such a comparison would be based ideally on an infinite number of tests in order to reduce the effects of scatter. Since this was not practicable, any analysis of the results must be made with the realization that the coverage is adequate but less than ideal.

In order to be as objective as possible on this point, the authors have made use of statistical analysis methods for the evaluation of the results. Basically, this involves:

(1) Arriving at the best single estimate of the difference between the mean of all mild steel values and the mean of all high yield steel values.

(2) Applying statistics to this best estimate to arrive at the limits within which we may rely on this particular value, based on a 95% confidence level.

(3) The application of confidence limits to the particular mean at each standoff for both the mild steel and the high yield steels in order to give a graphical presentation of the variation in the differences of the mean over the entire range of testing.

Each of these sections will be discussed in turn.

A. Analysis Based on Average Differences

(1) From the table of test energies, Table VI, the mean energy value for all plates at each of the four standoff positions is calculated. The difference between this mean at each standoff and the value for each individual plate at that standoff is then computed and plotted as an energy difference.

(2) All mild steel differences are then averaged to arrive at a common mean for that metal. The values for all high yield metals are averaged collectively in a similar manner. The plot of the means so derived provides a direct comparison.

(3) Calculations for this work are given in Table VII.

(4) These values are presented graphically as Figures XVI-a and XVI-b respectively.

The final result of this procedure is that the mean of all mild steel energies falls below the mean of all the energies for the high yield steels by a value of 695 foot-pounds. To test the engineering significance of this figure, we may apply it to the average energy of the high yield steels at a 5 foot standoff and express the differential

as a percentage strength increase for mild steel. Based on this average value of 22,300 foot-pounds, the 695 foot-pound differential represents a relative strengthening effect for mild steel of only 3.1%. The increase predicted by laboratory work with equivalent dynamic conditions was given in Chapter I as 20%. The results of this section then show that only 15% of the predicted effect can be established, and the conclusion is drawn that the relative strengthening effect for mild steel made evident by the calculations of this section is of no engineering significance.

TABLE VII

CALCULATION OF AVERAGE DIFFERENCE BETWEEN MILD STEEL AND HIGH YIELD STEELS

Stand off	Plate No.	Metal	x Energy	$\bar{x}$ Mean	$(x-\bar{x})$	Mild Steel Mean $(x-\bar{x})/n_{MS}$	High Yield Steels Mean $(x-\bar{x})/n_{HY}$
4 ft.	1	MS	37600	36230	+1370	-295	+ 400
	7	STS	35450		- 780		
	13	HY	35700		- 530		
	16	MS	37600		+1370		
	34	MS	34800		-1430		
5 ft.	2	MS	21410	21360	+ 50		
	8	STS	20200		-1160		
	14	HY	22500		+1140		
	17	MS	18230		-3130		
	21	STS	24180		+2820		
	31	MS	21300		- 60		
6 ft.	3	MS	11890	13736	-1846		
	9	STS	17800		+4064		
	15	HY	12270		-1466		
	25	STS	13500		- 236		
	33	MS	13060		- 676		
7 ft.	18	MS	9850	8242	+1608		
	27	STS	7350		- 892		
	30	MS	8170		- 72		
	32	MS	7800		- 442		

FIGURE XVI

Overall Difference Between Means of Mild and High Yield Steels

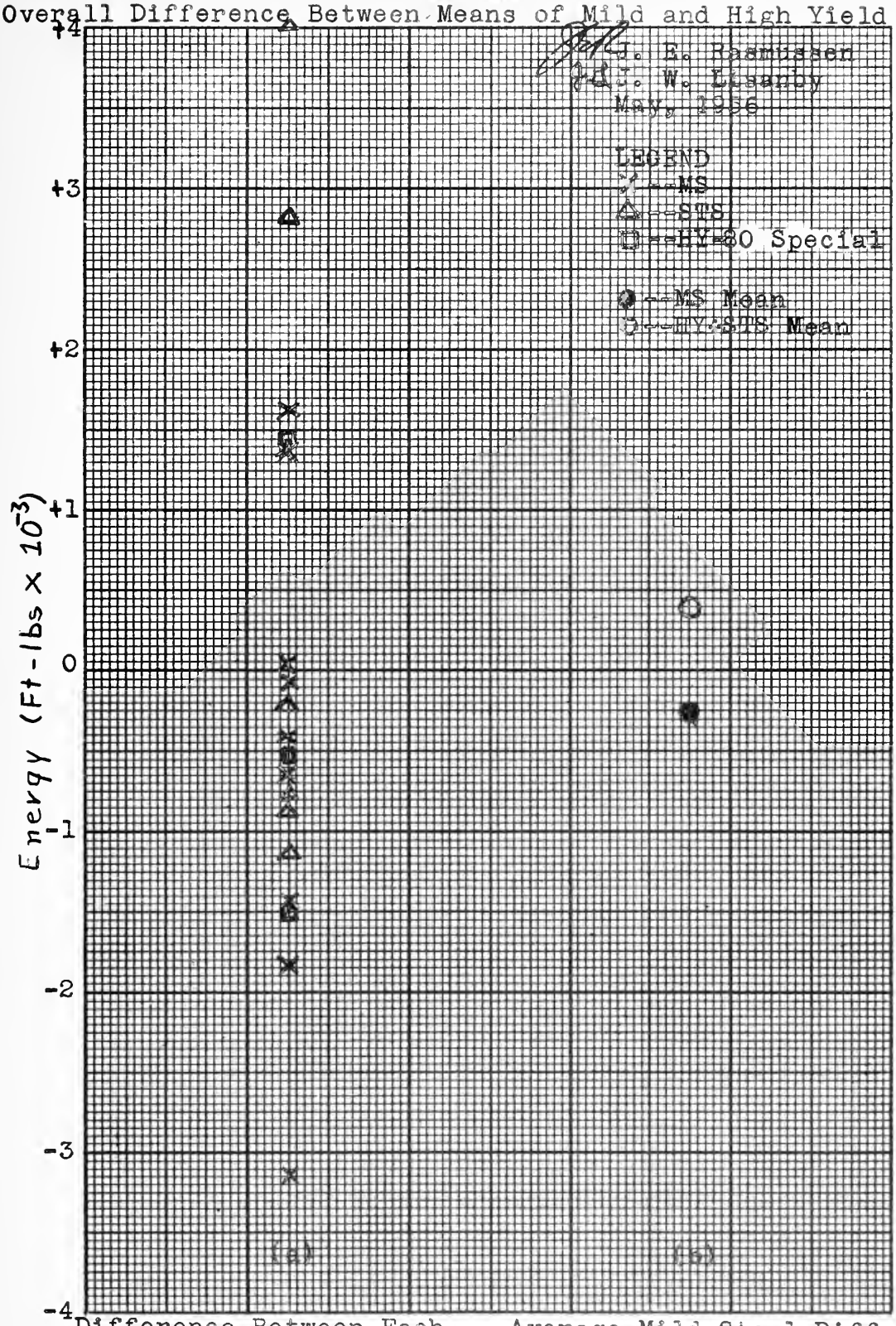

(a) Difference Between Each Energy and Mean Energy at That Standoff

(b) Average Mild Steel Difference and Average High Yield Difference

B. Confidence Limits to be Placed on the Value of Average Difference

The derivation of the confidence limits to be placed on the average difference between the mild steel mean and the high yield steel mean is carried out in Appendix E-1 because of its length, and the final result is given by the expression:

$$t = \frac{(\bar{x}_{HY} - \bar{x}_{MS}) - (\bar{X}_{HY} - \bar{X}_{MS})}{\sigma_R} \quad \frac{\sqrt{\nu}}{V} \qquad (30)$$

the component parts of which have also been evaluated in Appendix E-1 as:

$(\bar{x}_{HY} - \bar{x}_{MS}) = 695$ foot pounds (from Table VII)

$\sqrt{\nu} = 3.47$

$V = 6.31/\sigma$

$\sigma_R = 0.395\sigma$

$t = 2.18$ (based on 7 degrees of freedom and 95% confidence)

The equation may then be solved for the difference of the infinite population means, $(\bar{X}_{HY} - \bar{X}_{MS})$, which gives:

$$+2255 > \bar{X}_{HY} - \bar{X}_{MS} > -865$$

Statistically, this result implies that we may predict, with 95% confidence, that the true mean value of mild steel may fall within a band of from 865 foot-pounds over, to 2255 foot-pounds below the true mean value for the high yield steels.

From theoretical reasoning we may rule out the possibility that mild steel will exhibit a smaller relative strengthening effect than the high yield steels. This is contrary to all previous investigations and need not be

considered in this discussion.

If we consider the other extreme in which mild steel energy falls below the high yield steels by 2255 foot-pounds we can establish the maximum limit. For comparative purposes, the average energy of 22,300 foot-pounds for a 5 foot STS shot is again used. The value of 2255 foot-pounds then represents a relative strengthening effect for mild steel of 10%.

From the theoretical background given in Chapter I the average predicted effect was a 20% increase for mild steel. The conclusion of this section is then reached that even the extreme limiting value represents but half of the strengthening effect which is predicted for mild steel from laboratory experimentation and that the total effect is of no engineering significance.

The reader is cautioned that the numerical work of this section should be considered a qualitative rather than a quantitative measure of the relative strengthening because of the several simplifying assumptions necessarily used, the lack of complete data in several cases, and the particular uncertainties associated with underwater explosions.

C. Derivation of Confidence Bands for the Curve of the Mean

Statistical analysis is now used to set confidence limits on the curves of the mean energies for both mild steel and the high yield steels. These experimental bands may then be plotted together to show the distribution with stand-off of all probable energy differences which may exist

between mild steel and the high yield steels.

The use of this technique requires that we express the data in a form familiar to the statistician. This may be done as follows:

Let the calculated value of energy absorbed by each plate be represented by x. At each standoff these values may be assumed to have normal distribution, an infinite population mean of $\bar{X}$, and standard deviation from this mean of σ, where σ is assumed to be the same for all standoffs. The arithmetic mean of a sample of n_1 values taken from this population will then be normally distributed with a value of $\bar{x}$ and standard deviation $\sigma/\sqrt{n_1}$.

Symbolically, this statement may be presented:

$$(\bar{x}_1 - \bar{X}_1) \text{ is } N\left(0, \sigma/\sqrt{n_1}\right) \tag{31}$$

or

$$\frac{(\bar{x}_1 - \bar{X}_1)}{\sigma/\sqrt{n_1}} \text{ is } N(0, 1) \tag{32}$$

The detailed work for this procedure is presented in Appendix E-2 because of its length and subordinate nature. The final result is presented in Figure XVII. Figure XVII shows that the confidence bands for mild steel and high yield steel superimpose, in general, over the entire range. Since the true curve of mean energy for both the mild steel and the high yield steels, based on an infinite number of tests, may be anywhere within their limiting bands, it may be concluded that the difference is statistically insignificant and that mild steel exhibits no relative strengthening effect

of engineering significance with the strain rates found in underwater explosive loading of this intensity.

FIGURE XVII

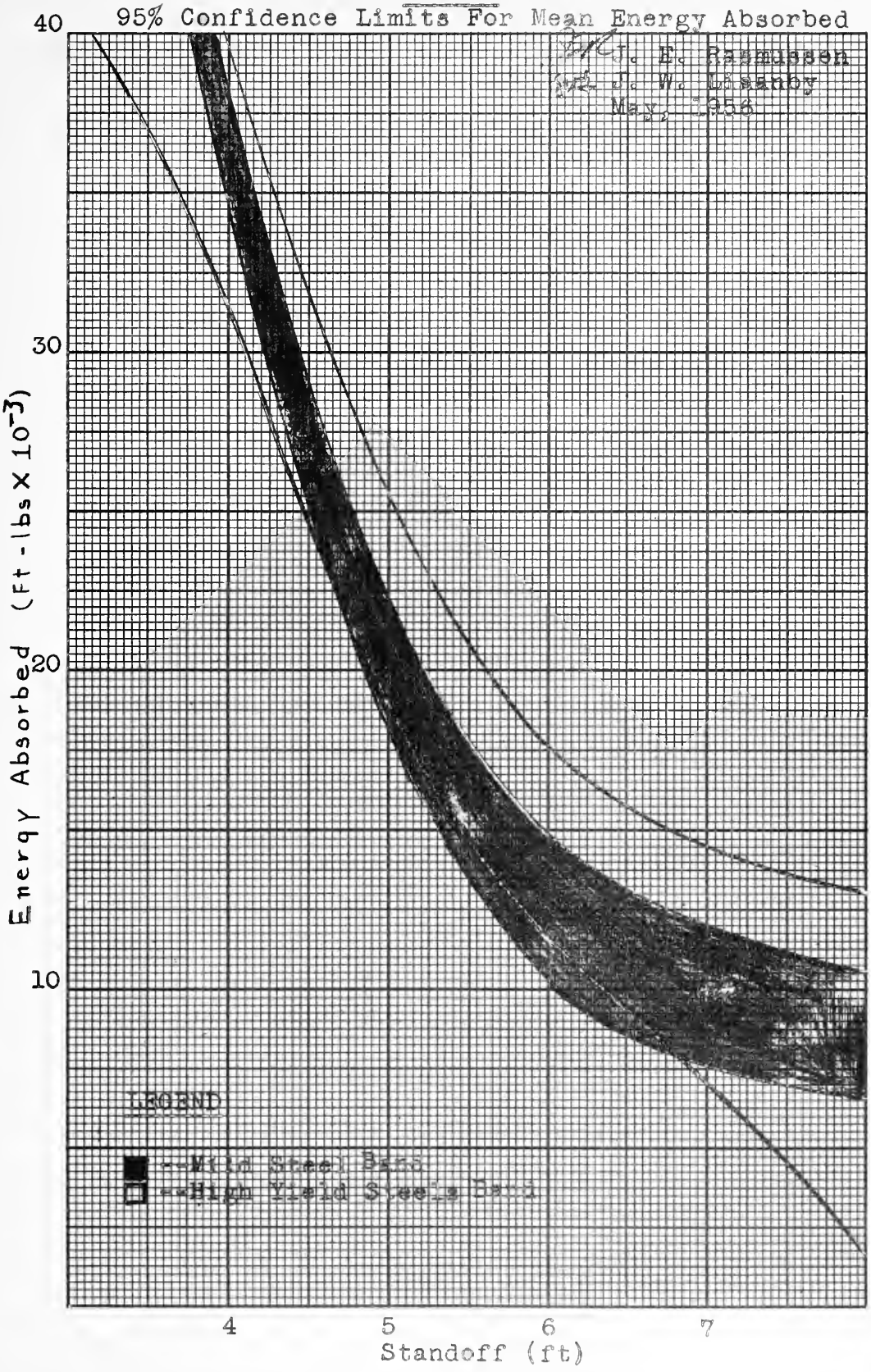
95% Confidence Limits For Mean Energy Absorbed
by J. E. Rasmussen
and J. W. Lisanby
May, 1956
Energy Absorbed (Ft-lbs X 10⁻³)
40
30
20
10
4
5
6
7
Standoff (ft)
LEGEND
--Mild Steel Bars
--High Yield Steel Bars

V. CONCLUSIONS

The final conclusion is drawn that, for the strain rates associated with underwater explosive loadings acting on simple, practical structures with normal surface imperfections and residual stresses, mild steel may exhibit greater strengthening than will a high yield steel. However, this relative strengthening effect of mild steel is less than that predicted from laboratory tests and is considered to be of no engineering significance. Predicted values of this relative effect run from 5% to 39%, whereas the observed values run from 0% to 10%.

It is further concluded that an adequate comparison of the relative dynamic strengths of such steels may be made based entirely on the static stress-strain relationships for the steels.

APPENDIX

APPENDIX A

NOMENCLATURE

A = Area of plate or element of plate

A_o = Original area

c = Speed of sound in water

D = Plate diameter

DY = Plate designation for project. Precedes all plate numbers.

E = Energy; E_e = Explosion energy

E_m = Distortion energy

E_b = Bending energy

h = Plate thickness

h_o = Original plate thickness

HY = High yield stress steels

I = Moment of inertia

K = Explosion parameter

l = Length of tension test pull specimen or distance along flat surface of plate

l_o = Original length

m = Mass of plate

M = Moment

M_o = Ultimate bending moment

r = Radius of plate distance from center

R = Distance (standoff) between charge and plate

T = Torque or moment

v = Velocity

V = Volume, $\triangle V$ is an increment of volume

Y = Young's Modulus

z = Deflection of plate from original plane

Z = Section modulus

$\bar{\delta}$ = Effective strain

$\bar{\varepsilon}$ = Engineering strain

ε = Logarithmic strain

ρ = Density of water

$\bar{\sigma}$ = Engineering stress

σ = True stress

σ_d = Dynamic stress

σ_y = Normal lower yield stress

APPENDIX B

DETAILS OF PROCEDURE

Several methods for calculation of plate energies were attempted. They vary greatly in complexity and accuracy. In this appendix a brief description of each method will be presented and its results analyzed.

1. Calculation of Membrane Energy by Theoretically Correct Method.

In order to check the validity of the method for energy determination used by the authors, $\frac{E}{V} = \int \sigma_h d\varepsilon_h$, a comparison was made with a more exact method presented by Smith, page 58 (23). Smith's method is theoretically more accurate in that it includes the refinement that radial strain need not equal circumferential strain.

The application of the method requires that we evaluate an "effective strain," $\bar{\delta}$, defined by the radical:

$$\bar{\delta} = \sqrt{\frac{2}{3}\left(\delta_r^2 + \delta_\theta^2 + \delta_h^2\right)}$$

where: $\delta_r = \ln\frac{r}{r_o}$ = radial strain

$\delta_\theta = \ln\frac{c}{c_o}$ = circumferential strain

$\delta_h = \ln h/h_o$ = thickness strain

By use of the relation pertaining to constant volume: $\delta_r + \delta_\theta + \delta_h = 0$, this simplifies to

$$\bar{\delta} = \sqrt{2/3\,(2\delta_r^2 + 2\delta^2_h + 2\delta_r\delta_h)}$$

This radical is then evaluated by incremental steps and used to enter the stress-strain curves to obtain the "effective stress," $\bar{\sigma}$. Membrane energy is then found by the expression,

$$E = V\int \bar{\sigma}\, d\bar{\delta}$$

All calculations for this method are included in Tables B-1, B-2, B-3, for three mild steel plates. The three energies so obtained may then be compared with the cor-

responding values obtained by using the thesis method. This comparison is made in Figure B-1.

TABLE B-1

CALCULATION OF MEMBRANE ENERGY BY

EFFECTIVE STRESS-STRAIN METHOD

TEST DY-1

h_o = 0.252

R	δ_h	δ_r	$\bar{\delta}$	$\int \bar{\sigma} d\bar{\delta}$ x 10^3	ΔV	ΔE x 10^3
0	.470	.235	.4715		0	
0.5	.405	.203	.4058	1.940	.442	.8575
1.0	.348	.157	.3494	1.660	.785	1.3031
1.5	.293	.133	.2937	1.378	1.178	1.6233
2.0	.248	.117	.2487	1.152	1.571	1.8098
2.5	.207	.108	.2076	.942	1.963	1.8550
3.0	.178	.099	.1786	.800	2.356	1.8848
3.5	.156	.091	.1576	.697	2.749	1.9161
4.0	.138	.085	.1394	.608	3.142	1.9103
4.5	.124	.080	.1261	.542	3.534	1.9154
5.0	.113	.075	.1154	.480	3.927	1.8850
5.5	.100	.070	.1029	.430	4.320	1.8576
6.0	.091	.066	.0945	.380	4.712	1.7906
6.5	.082	.063	.0862	.354	5.105	1.8072
7.0	.073	.059	.0782	.315	5.498	1.7319
7.5	.065	.056	.0704	.280	5.890	1.6492
8.0	.060	.055	.0664	.262	6.283	1.6462
8.5	.049	.056	.0609	.238	6.676	1.5889
9.0	.041	.058	.0599	.231	7.069	1.6329
9.5	.049	.064	.0670	.264	7.461	1.9697
10.0	.051	.073	.0751	.300	3.874	1.1622
						E = 33,798.5

δ_r = radial strain = $\ln \frac{r}{r_o}$ (in/in)

δ_h = thickness strain = $\ln \frac{h}{h_o}$ (in/in)

$\bar{\delta}$ = effective strain = $\sqrt{\frac{2}{3}(2\delta_r^2 + 2\delta_h^2 + 2\delta_r\delta_h)}$

ΔV = increment of volume (in^3)

ΔE = increment of Membrane Energy (ft - lb)

TABLE B-2

CALCULATION OF MEMBRANE ENERGY BY

EFFECTIVE STRESS-STRAIN METHOD

TEST DY-2

$h_o = .2514$

R	δ_h	δ_r	$\bar{\delta}$	$\int \bar{\sigma} d\bar{\delta} \times 10^3$	ΔV	$\Delta E \times 10^{-3}$
0	.1970	.0950	.1974		0	0
0.5	.1920	.0913	.1926	.872	.442	.3854
1.0	.1680	.0766	.1683	.751	.785	.5934
1.5	.1480	.0665	.1485	.651	1.178	.7692
2.0	.1300	.0566	.1306	.564	1.571	.8860
2.5	.1130	.0505	.1136	.480	1.963	.9422
3.0	.0990	.0458	.0993	.416	2.356	.9801
3.5	.0865	.0430	.0867	.355	2.749	.9759
4.0	.0770	.0420	.0772	.310	3.142	.9740
4.5	.0684	.0414	.0690	.273	3.534	.9648
5.0	.0630	.0403	.0639	.248	3.927	.9739
5.5	.0586	.0392	.0605	.237	4.320	1.0239
6.0	.0555	.0382	.0569	.218	4.712	1.0272
6.5	.0545	.0368	.0556	.210	5.105	1.0720
7.0	.0545	.0355	.0554	.208	5.498	1.1436
7.5	.0523	.0348	.0534	.202	5.890	1.1898
8.0	.0480	.0351	.0497	.186	6.283	1.1686
8.5	.0440	.0367	.0473	.176	6.676	1.1750
9.0	.0377	.0400	.0450	.164	7.069	1.1593
9.5	.0315	.0448	.0461	.170	7.461	1.2684
10.0	.0253	.0515	.0516	.194	3.874	.7516

$E = 19,418.1$

δ_r = radial strain = $\ln \frac{r}{r_o}$ (in/in)

δ_h = thickness strain = $\ln \frac{h}{h_o}$ (in/in)

$\bar{\delta}$ = effective strain = $\sqrt{\frac{2}{3}(2\delta_r^2 + 2\delta_h^2 + 2\delta_r\delta_h)}$

ΔV = increment of volume (in^3)

ΔE = increment of Membrane Energy (ft - lb)

TABLE B-3

CALCULATION OF MEMBRANE ENERGY BY

EFFECTIVE STRESS-STRAIN METHOD

TEST D-3

$h_o = .2527$

R	δ_h	δ_r	$\bar{\delta}$	$\int \bar{\sigma} d\bar{\delta} \times 10^3$	ΔV	$\Delta E \times 10^3$
0	.1440	.0670	.1442		0	0
0.5	.1360	.0615	.1365	.594	.442	.2626
1.0	.1160	.0506	.1168	.498	.785	.3909
1.5	.0942	.0429	.0945	.392	1.178	.4476
2.0	.0770	.0376	.0767	.313	1.571	.4917
2.5	.0682	.0343	.0684	.270	1.963	.5300
3.0	.0630	.0316	.0631	.246	2.356	.5796
3.5	.0567	.0305	.0568	.217	2.749	.5965
4.0	.0502	.0295	.0506	.190	3.142	.5970
4.5	.0450	.0285	.0457	.168	3.534	.5937
5.0	.0388	.0282	.0403	.148	3.927	.5812
5.5	.0346	.0280	.0369	.131	4.320	.5659
6.0	.0315	.0274	.0343	.122	4.712	.5949
6.5	.0274	.0260	.0309	.110	5.105	.5616
7.0	.0274	.0246	.0302	.108	5.498	.5938
7.5	.0233	.0237	.0272	.098	5.890	.5772
8.0	.0212	.0232	.0258	.091	6.283	.5718
8.5	.0212	.0241	.0263	.095	6.676	.6342
9.0	.0212	.0258	.0276	.099	7.069	.6998
9.5	.0192	.0280	.0286	.102	7.461	.7610
10.0	.0050	.0334	.0361	.129	3.874	.4997

$E = 11,244$

δ_r = radial strain = $\ln \frac{r}{r_o}$ (in/in)

δ_h = thickness strain = $\ln \frac{r}{h_o}$ (in/in)

$\bar{\delta}$ = effective strain = $\sqrt{\frac{2}{3}(2\delta_r^2 + 2\delta_h^2 + 2\delta_r\delta_h)}$

ΔV = increment of volume (in^3)

ΔE = increment of Membrane Energy (ft - lb)

FIGURE B-1

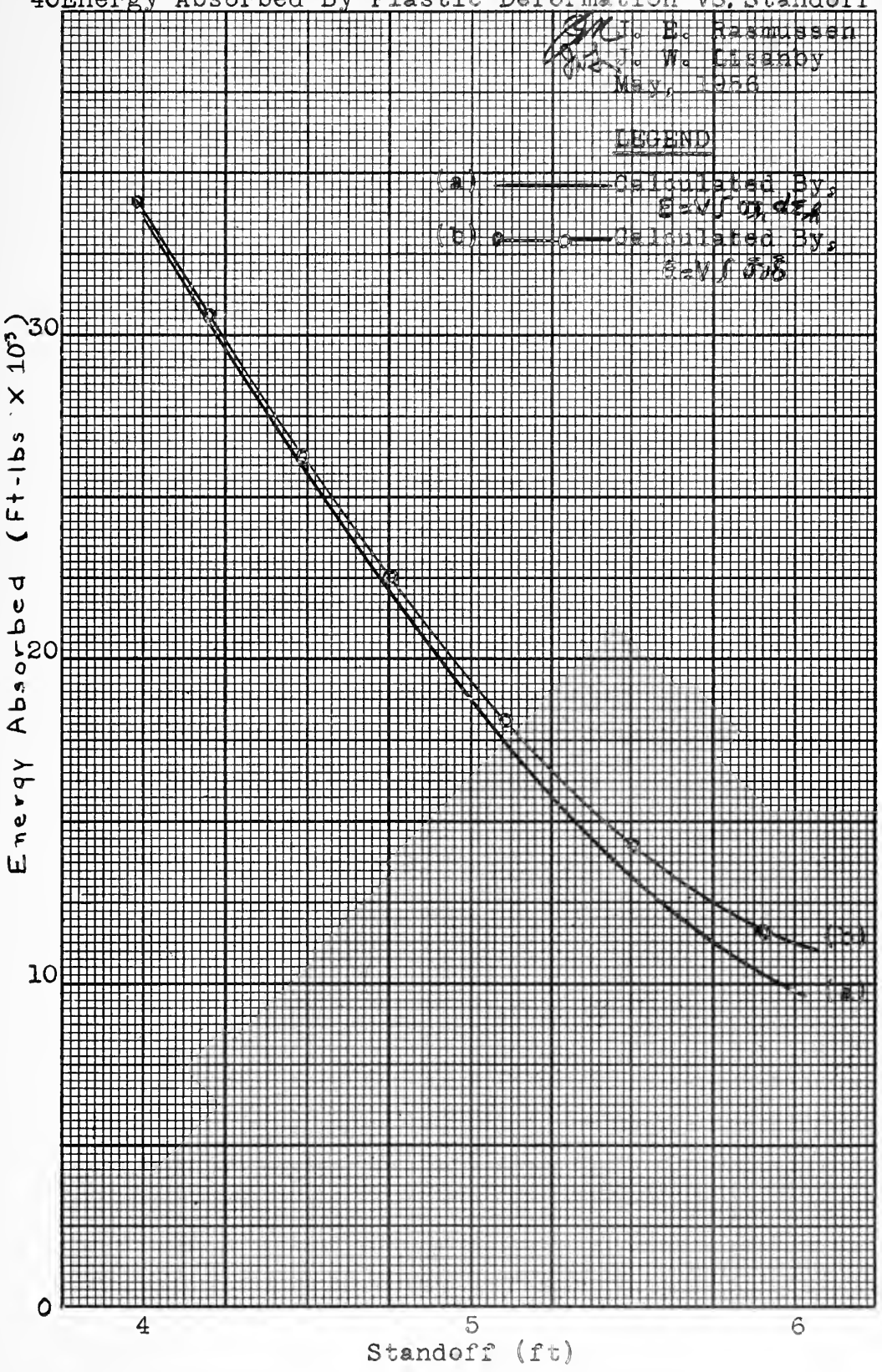
Energy Absorbed By Plastic Deformation VS. Standoff
J. E. Rasmussen
J. W. Lisenby
May, 1956
LEGEND
(a) Calculated By, $E = V \int \sigma_1 \, d\varepsilon_1$
(b) Calculated By, $E = V \int \bar{\sigma} \, d\bar{\varepsilon}$
Energy Absorbed (Ft-lbs X 10^3)
40
30
20
10
0
4
5
6
Standoff (ft)

2. Calculation of Energies by Use of an Area Strain.

Several papers have been written using the square of the deflection as a measure of strain. Thus,

$$E = Kh_o \sigma_y Z_c^2 \qquad \text{(B-1)}$$

where Z_c is the deflection of the center, σ_y is the lower yield stress, and K is a constant depending on the final shape of the plate. This equation is used to approximate a form where strain is represented by the ratio of change in area over the original area.

$$\varepsilon_A = \frac{\Delta A}{A}$$

$$E = Ah \int \sigma \, d\varepsilon_A = Ah \sigma_y \frac{\Delta A}{A} = h \Delta A \sigma_y \qquad (20)$$

K represents the value of the first term in the expansion of standard contour areas:

$K = \pi$ for a paraboloid of revolution

$K = \pi/2$ for a cone

Since final explosive shapes are neither paraboloids nor cones, the theoretical accuracy of this method is questionable even at small deflections. As deflections increase, accuracy decreases.

This is a very simple method for estimating energy, however, and its accuracy should be investigated. Figure B-II shows a plot of dA versus Z_c. The values of $dA = A - A_o$ were determined by graphical integration based on

$$A = \sum_{r=\frac{1}{2}}^{r=10} 2\pi r \, ds \qquad \text{(B-2)}$$

FIGURE B-II

Deflection squared versus change in area of plate.

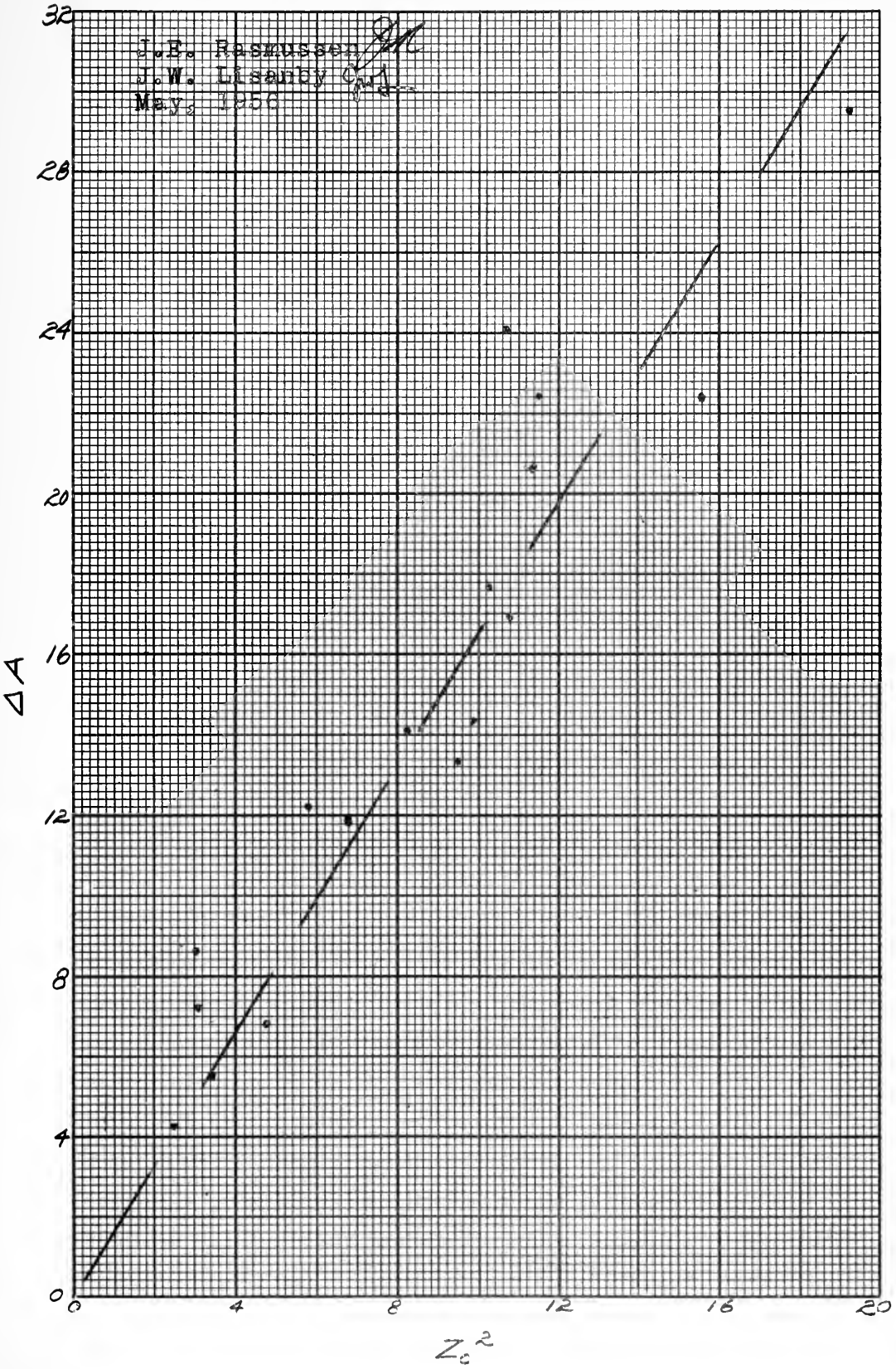

Figure B-III pictures this method.

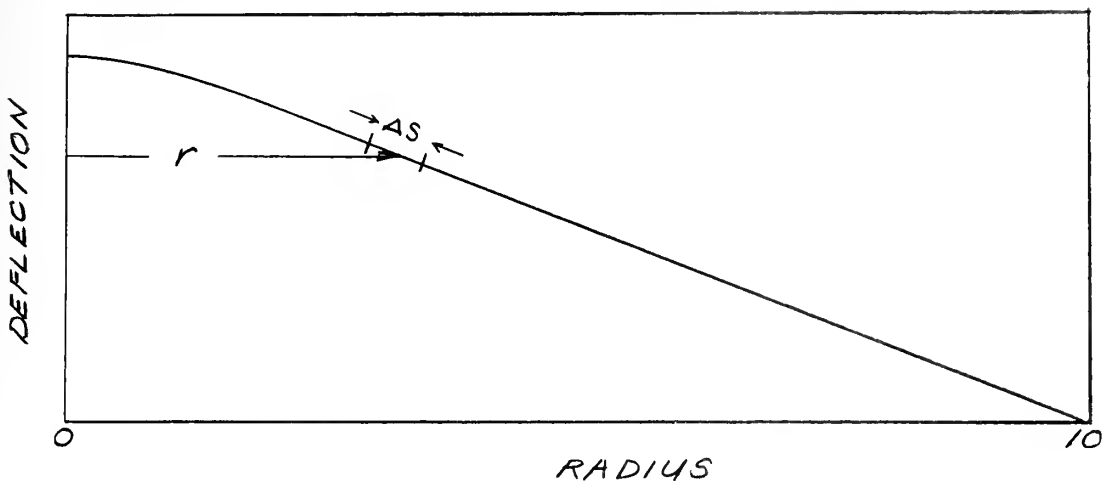

Figure B-III

Deflection Versus Radius for Computing Area of Plates

Table B-IV shows such a calculation for DY-1. Table B-V also shows a compilation of deflection, ΔA, and energies computed in different ways, for each plate tested.

ΔE is an energy per unit volume taken from the stress-strain curve with the average strain $\varepsilon_A = \Delta A/A_o$ as argument. This value multiplied by the total plate volume is E_1. E_2 is formed by taking the value of stress from the curve for strain $= \frac{\Delta A}{A_o}$.

$$E_2 = V \sigma_A \varepsilon_A \qquad \text{(B-5)}$$

Assuming the values of energy from thickness strains are correct, we see that the large errors in the energies computed with area stresses render the method of dubious value in explosive distortion energy calculations.

Values of energy computed by equation (B-5) are plotted in Figure B-IV. The curve is for average thickness energies used in the body of the report.

TABLE B-IV

CALCULATION OF INCREASED AREA

DY-1

r	ds	rds
0		
.5	.505	.126
1	.52	.390
1.5	.54	.675
2	.545	.953
2.5	.55	1.237
3	.56	1.540
3.5	.565	1.836
4	.56	2.100
4.5	.56	2.380
5	.558	2.650
5.5	.55	2.887
6	.55	3.162
6.5	.55	3.437
7	.56	3.780
7.5	.57	4.132
8	.58	4.495
8.5	.57	4.702
9	.56	4.900
9.5	.55	5.087
10	.55	5.362

$A/2\pi = 55.831$

$A = 350.796$

$A_o = 314.159$

$dA = 36.637$

TABLE B-V

COMPARISON OF ENERGIES BY AREA STRAIN METHOD WITH THICKNESS STRAIN METHOD

DY	Z_c^2	dA	E_1	% Error	E_2	E_Z	% Error
1	20.50	36.64	39,100	15.9	41,700	34,500	2.4
2	10.25	17.61	16,750	-10.8	19,050	17,230	- 8.2
3	6.77	11.94	10,680	8.4	11,940	11,400	13.6
4	10.40	-----				28,200	
5	9.85	14.30				26,700	
6	19.20	29.56				52,000	
7	9.50	13.33	31,650	- 2.4	32,650	43,600	41.2
8	4.75	6.81	16,040	- 2.3	16,040	21,800	33.0
9	2.50	4.25	9,810	-33.8	9,970	11,500	-22.3
10	11.55	22.44	22,500	15.7	25,400	21,600	10.8
11	22.20	25.49	38,500	- 6.6	45,350	41,500	0.7
12	8.20	14.15	13,500	19.3	14,280	15,300	35.4
13	10.70	24.09	49,300	63.9	51,700	39,800	32.2
14	5.80	12.24	24,300	31.3	24,900	21,500	16.2
15	3.45	5.47	10,770	1.6	10,680	12,800	38.2
16	19.75	32.67	36,390	7.9	45,900	38,000	8.3
17	11.35	20.66	21,200	34.0	24,650	21,900	38.6
18	5.02	8.60	8,400	- 0.9	8,430	9,700	16.8
19	---	---	---				
20	15.60	22.44	49,100	- 4.4	51,600	61,800	20.5
21	5.12	7.19	14,700	-27.7	15,100	20,300	0

% Error based on values of energy $E = V\int \sigma_h d\varepsilon_h$ of Table VI.

FIGURE B-IV

E_A VS Standoff

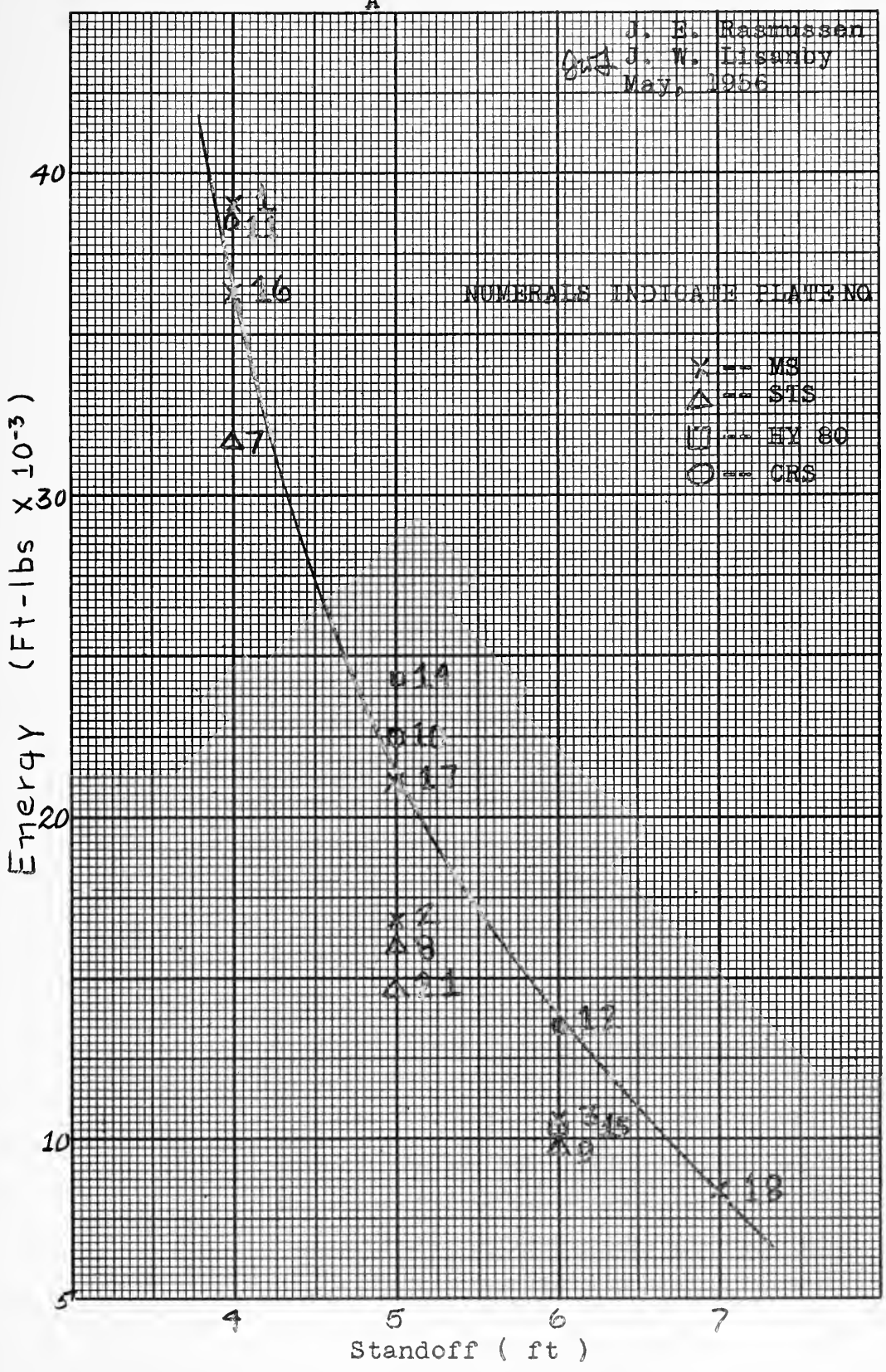

E_Z is an energy calculated using equation (B-3) where K is the slope of the average faired line of Figure B-II.

$$K = \frac{\Delta A}{Z_c^2} = 1.64$$

$$E_Z = 1.64\ h_o \sigma_Z Z_c^2 \qquad \text{(B-6)}$$

Values of σ_Z were initial lower yield stresses.

Values of energy computed from (B-6) are plotted in Figure B-V. The curve is again that for average thickness energy.

It should be noted that although the energies fall around the thickness average, they are very erratic and undependable.

FIGURE B-V

E_z VS Standoff

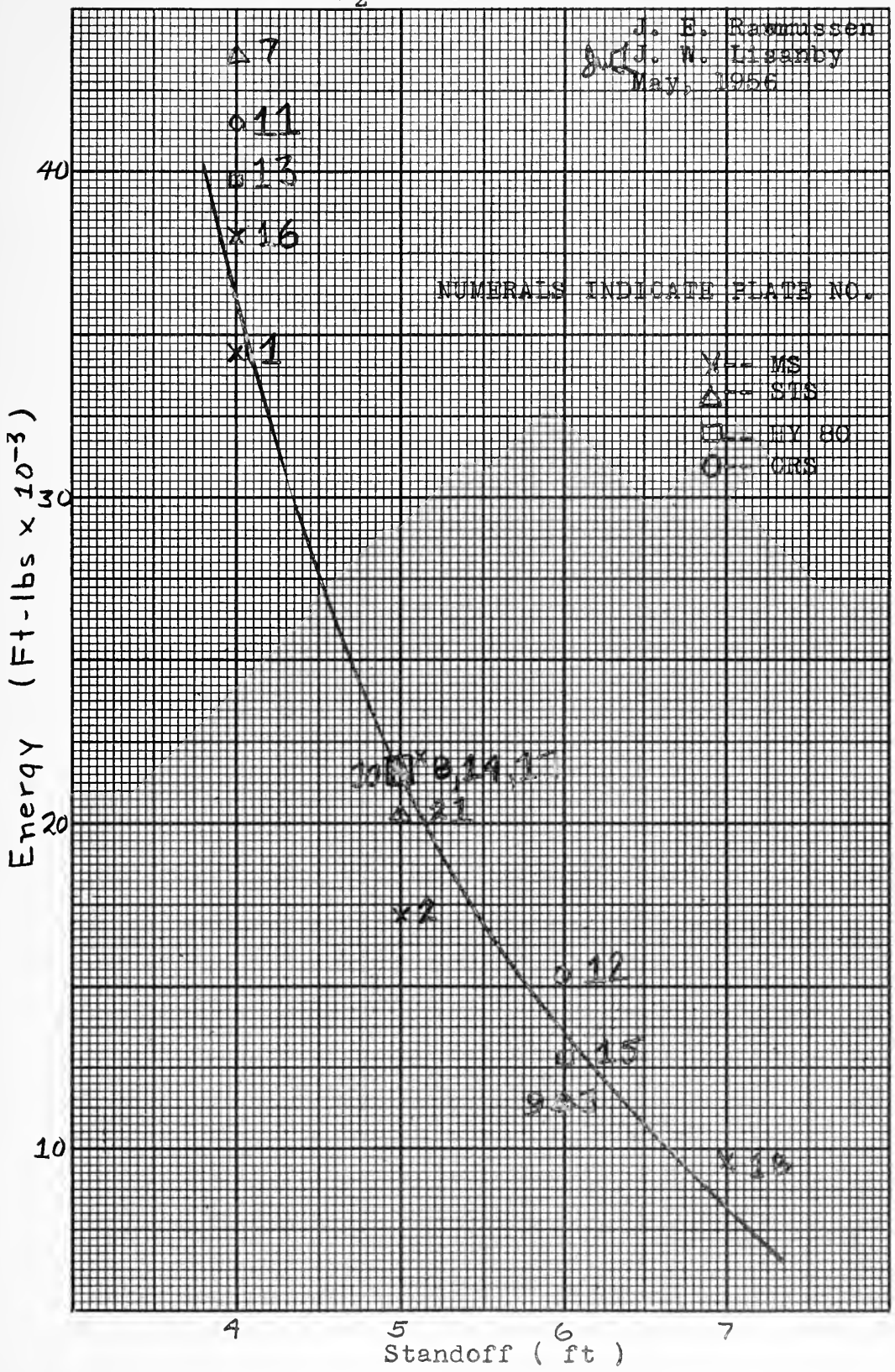

3. Calculation of Energies by Biaxial Strain.

Since actual strains are biaxial in the plane of the plate, a possible method of calculating plate energy is:

$$\frac{E}{V} = \int \sigma_r d\varepsilon_r + \int \sigma_\theta d\varepsilon_\theta$$

where: ε_r = radial strain

ε_θ = circumferential strain

We computed six plates in this method using engineering strains based on punch marks. Radial strain was determined by the increase in distance between punch marks. Circumferential strain may be computed directly from the outward radial movement of punch marks from the center:

$$\varepsilon_\theta = \frac{\Delta r}{r} \qquad \text{(B-7)}$$

Or it may be computed using the more accurate thickness and radial strain measurements where:

$$(1 + \varepsilon_\theta)(1 + \varepsilon_r)(1 + \varepsilon_h) = 1 \qquad \text{(B-8)}$$

ε_θ values computed by equation (B-8) were used.

Compilation of results is in Table VI. These energies are plotted in Figure B-VI with a curve of thickness energies (see Figure XV).

TABLE VI

ENERGIES COMPUTED BY BIAXIAL STRAINS

Plate	Biaxial Energy
DY-1	33,214
2	15,382
3	9,993
7	32,750
8	16,884
9	10,080

The consistency of these results make it seem acceptable for use in energy calculations. It should be noted that bending energy has not been added to the "biaxial" energies in Figure B-VI.

FIGURE B-VI
Biaxial Energy VS Standoff

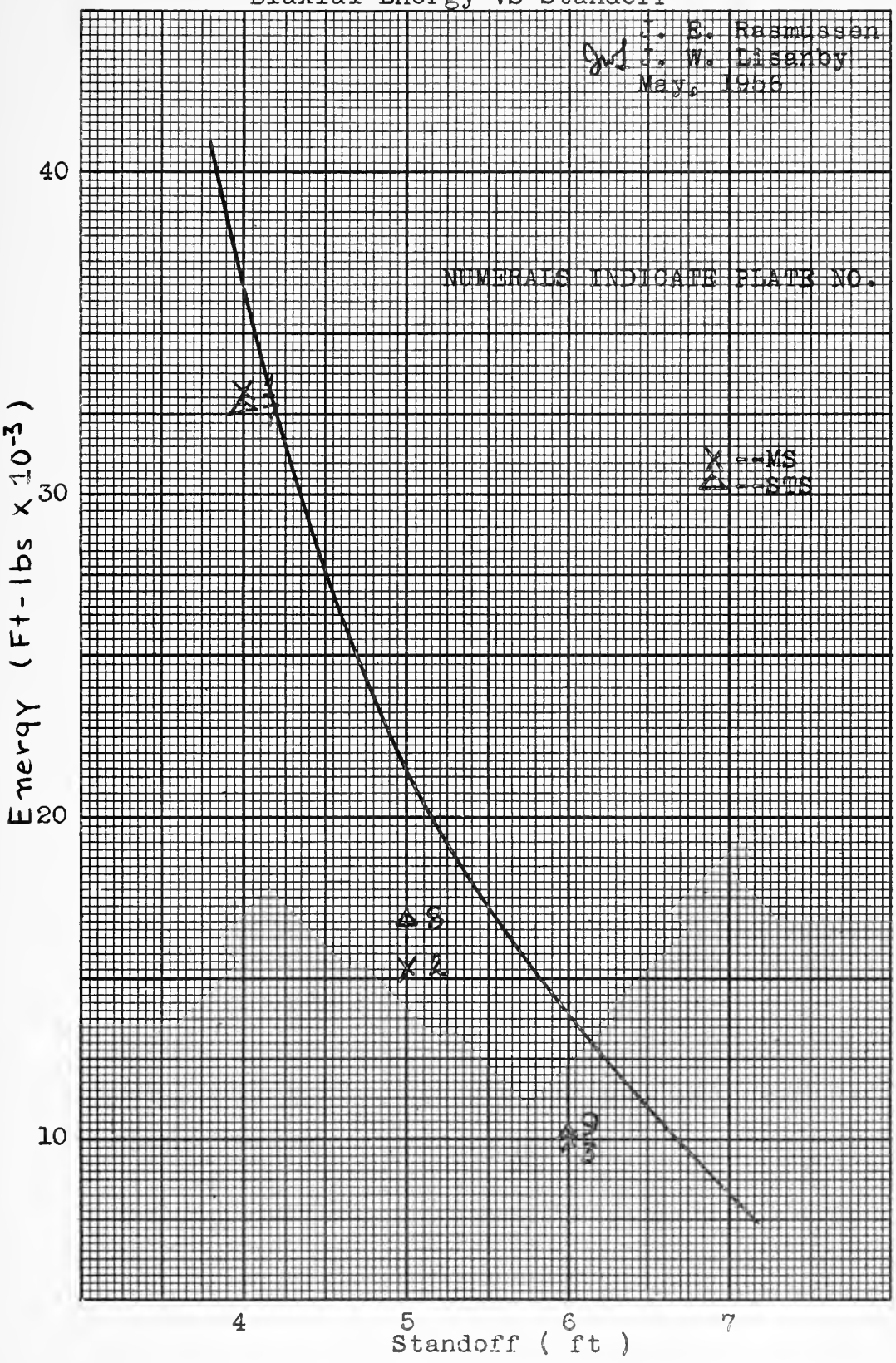

APPENDIX C

SUMMARY OF ORIGINAL DATA

Original data for all tests is stored in the files of the Underwater Explosions Research Division, Norfolk Naval Shipyard, Portsmouth, Virginia. Extensive data were taken. Only summaries of that data which was used in the main body of the thesis is presented here in the interest of brevity. Samples of original data for two plates are included in Appendix F to illustrate the method of gathering data and the degree of anisotropy.

1. Averages of Original Data for Plates.

Plates shot in this series of tests had the below readings taken on them. These readings were summarized as follows:

a. Each plate had its deflection read along four radii before and after each shot. These four readings were averaged at each radius and tabulated in the summary.

b. Most plates (26 plates) were sawed in two along a diameter after being shot. Thickness readings were taken along two radii. These two readings are averaged and tabulated in the summary.

c. Thirteen plates were marked with two-inch punch marks along two diameters. Measurements were made before and after the explosion to determine the change in distance between these punch marks. All four changes in distance, Δs, are recorded as arithmetic averages.

d. The movement of punch marks away from the center as the plate deflected were made on some plates. Where tabulated, these are averages of four readings at each radius. These readings were quite inaccurate and not used in the final analyses.

2. Data for Plotting Stress-Strain Curves.

In order to obtain sufficient data to allow plotting a curve of true stress versus true strain in the region of yielding, special tensile tests were conducted. In these tests all specimens were turned down to a diameter of approximately 0.225 inch. While tests were being pulled, diameter readings were taken every .025 inch per 2-inch elongation. This allowed computation of instantaneous

stress:

$$\sigma = \frac{F}{A}$$

and actual strain in the region of plastic deformation:

$$\varepsilon = \ln \frac{l}{l_o} = \ln \frac{A_o}{A}$$

where $A = \frac{\pi d^2}{4}$

TABLE C-I

SUMMARY OF ORIGINAL DATA

DY-1		h_o = 0.2520			DY-2		h_o = .2514		
R_o	z	h	R	ds	R_o	z	h	R	ds
0	4.525	.1575		.3748	0	3.205	.2065		.1480
¼					¼		.2055		
½		.168			½		.210		
1	4.355		1.117		1	3.12	.2145	1.031	
2	3.955	.1967		.2478	2	2.87	.223		.1190
3	3.49	.2200	3.219		3	2.53	.2267	3.031	
4	2.95			.1780	4	2.18	.2337		.0860
5	2.44	.230	5.144		5	1.82	.2365	5.055	
6	1.98			.1296	6	1.48	.238		.0780
7	1.50	.2375	7.059		7	1.13	.238	7.101	
8	1.03			.1100	8	0.78	.240		.0708
9	0.58		8.976		9	0.45	.243		
10	0.11	.2397		.1522	10	0.09	.2462		.1046

All measurements are in inches.

R_o = Original radius

R = Radius after deformation

h_o = Original thickness

h = Thickness after distortion

z = Deflection

ds = Increase in distance between 2-inch punch marks

TABLE C-II

SUMMARY OF ORIGINAL DATA

DY-3		h_o = 0.2527			DY-22		h_o = 0.2512		
R_o	z	h	R	ds	R_o	z	h	R	ds
0	2.605	.219		.0970	0	3.29	.201		
¼		.2195			¼		.2025		
½		.2205			½		.2055		
1	2.535	.225	1.047		1	3.18	.2135	1.086	
2	2.32	.2342		.0764	2	2.91	.222		.1116
3	2.055	.237	3.050		3	2.56	.230	3.101	
4	1.765	.2405		.0604	4	2.20	.235		.0836
5	1.465	.2427	5.039		5	1.83	.2385	5.072	
6	1.19	.2445		.0558	6	1.47	.241		.0730
7	0.905	.2457	7.012		7	1.12	.2415	7.031	
8	0.625	.2475		.0464	8	0.79	.2445		.0620
9	0.365	.2475			9	0.46	.2455		
10	0.095	.2515		.0670	10	0.12	.249		.1090

All measurements are in inches.

R_o = Original radius

R = Radius after deformation

h_o = Original thickness

h = Thickness after distortion

z = Deflection

ds = Increase in distance between 2-inch punch marks

TABLE C-III

SUMMARY OF ORIGINAL DATA

DY-7 Original thickness = h_o = 0.2480

R_o	z	h	R	ds
0	3.085	.194		.1912
¼		.1942		
½		.2010		
1	2.96	.2072	1.078	
2	2.67	.2210		.1128
3	2.34	.2282	3.101	
4	1.98	.2322		.0787
5	1.62	.2360	5.062	
6	1.29	.2380		.0564
7	0.97	.2417	7.016	
8	0.63	.2437		.0439
9	0.38	.2427	8.961	
10	0.09	.2490		.0761

DY-8 Original thickness = h_o = 0.2536

R_o	z	h	R	ds
0	2.18	.2225		.0834
¼		.2235		
½		.2265		
1	2.095	.2307	1.055	
2	1.885	.2375		.0576
3	1.63	.2425	3.062	
4	1.37	.2465		.0412
5	1.12	.2475	5.023	
6	0.88	.2482		.0332
7	0.65	.2487	6.992	
8	0.435	.2495		.0252
9	0.23	.2520	8.953	
10	0.04	.2535		.0504

All measurements are in inches.

R_o = Original radius

R = Radius after deformation

h_o = Original thickness

h = Thickness after distortion

z = Deflection

ds = Increase in distance between 2-inch punch marks

TABLE C-IV

SUMMARY OF ORIGINAL DATA

DY-9 h_o = 0.2538 Original thickness = h_o = 0.2538

R_o	z	h	R	ds
0	1.58	.2337		.0408
¼		.2337		
½		.2362		
1	1.51	.2407	1.023	
2	1.36	.2447		.0228
3	1.19	.2460	3.023	
4	1.01	.2465		.0210
5	0.82	.2470	5.008	
6	0.63	.2475		.0196
7	0.485	.2482	7.008	
8	0.34	.2505		.0106
9	0.18	.2520	8.984	
10	0.03	.2530		.0280

All measurements are in inches.

R_o = Original radius

R = Radius after deformation

h_o = Original thickness

h = Thickness after distortion

z = Deflection

ds = Increase in distance between 2-inch punch marks

TABLE C-V

SUMMARY OF ORIGINAL DATA

DY-4 R_o	z	h
0	3.22	
¼		
½		
1	3.13	
2	2.87	
3	2.54	
4	2.17	
5	1.80	
6	1.45	
7	1.11	
8	0.77	
9	0.45	
10	0.12	

NOT TAKEN

DY-5 R_o	h_o = 0.2265 z	h
0	3.14	.197
¼		
½		
1	3.04	.188
2	2.74	.198
3	2.42	.205
4	2.06	.210
5	1.71	.215
6	1.37	.217
7	1.04	.218
8	0.72	.219
9	0.40	.221
10	0.09	.224

DY-6 R_o	h_o = 0.2266 z	h
0	4.38	0.129
¼		.136
½		.1445
1	4.20	.159
2	3.84	.175
3	3.36	.1875
4	2.87	.196
5	2.36	.204
6	1.88	.208
7	1.43	.211
8	0.99	.217
9	0.56	.2175
10	0.13	.2205

DY-10 R_o	h_o = .2455 z	h
0	3.59	.196
¼		.197
½		.199
1	3.46	.204
2	3.19	.2115
3	2.82	.218
4	2.43	.2235
5	2.03	.228
6	1.63	.232
7	1.25	.2345
8	0.87	.2375
9	0.50	.2385
10	0.12	.242

All measurements are in inches.

R_o = Original radius

R = Radius after deformation

h_o = Original thickness

h = Thickness after distortion

z = Deflection

ds = Increase in distance between 2-inch punch marks

TABLE C-VI

SUMMARY OF ORIGINAL DATA

DY-11 h_o = 0.2485

R_o	z	h
0	4.70	.172
¼		.1732
½		.1755
1	4.56	.1847
2	4.15	.1952
3	3.68	.202
4	3.16	.2097
5	2.64	.2167
6	2.14	.2225
7	1.64	.229
8	1.15	.2335
9	0.65	.2365
10	0.15	.2422

DY-12 h_o = 0.2535

R_o	z	h
0	2.86	.220
¼		.221
½		.223
1	2.77	.2265
2	2.55	.231
3	2.27	.2355
4	1.97	.239
5	1.63	.2425
6	1.32	.244
7	1.02	.2465
8	0.71	.248
9	0.41	.249
10	0.11	.2515

DY-13 h_o = 0.2577

R_o	z	h
0	3.27	.1925
¼		.1972
½		.2052
1	3.13	.2127
2	2.85	.2235
3	2.49	.2325
4	2.12	.2395
5	1.74	.243
6	1.38	.247
7	1.03	.249
8	0.72	.252
9	0.41	.2532
10	0.10	.2585

DY-14 h_o = 0.2584

R_o	z	h
0	2.41	0.222
¼		.2235
½		.226
1	2.32	.2315
2	2.10	.239
3	1.84	.242
4	1.58	.246
5	1.30	.249
6	1.04	.2515
7	0.78	.2525
8	0.55	.255
9	0.33	.255
10	0.10	.257

All measurements are in inches.

R_o = Original radius

R = Radius after deformation

h_o = Original thickness

h = Thickness after distortion

z = Deflection

ds = Increase in distance between 2-inch punch marks

TABLE C-VII

SUMMARY OF ORIGINAL DATA

DY-15 h_o = 0.2581

R_o	z	h
0	1.86	.233
¼		.233
½		.2345
1	1.78	.238
2	1.61	.244
3	1.39	.249
4	1.20	.2515
5	0.99	.2535
6	0.77	.2545
7	0.57	.255
8	0.37	.257
9	0.24	.2575
10	0.04	.2590

DY-16 h_o = 0.2459

R_o	z	h
0	4.445	.150
¼		.156
½		.164
1	4.31	.174
2	3.93	
3	3.44	.207
4	2.93	.2155
5	2.44	.222
6	1.95	.2255
7	1.48	.2305
8	1.03	.231
9	0.58	.232
10	0.145	.2384

DY-17 h_o = 0.248

R_o	z	h
0	3.37	.199
¼		.202
½		.205
1	3.265	.210
2	2.97	.219
3	2.615	.227
4	2.24	.231
5	1.87	.235
6	1.49	.239
7	1.125	.240
8	0.77	.241
9	0.43	.237
10	0.085	

DY-18 h_o = 0.2456

R_o	z	h
0	2.24	.218
¼		.2185
½		.221
1	2.16	.2235
2	1.97	.2305
3	1.74	.2315
4	1.49	.235
5	1.24	.2385
6	1.00	.2415
7	0.76	.2415
8	0.52	.242
9	0.30	.241
10	0.07	.2445

All measurements are in inches.

R_o = Original radius

R = Radius after deformation

h_o = Original thickness

h = Thickness after distortion

z = Deflection

ds = Increase in distance between 2-inch punch marks

TABLE C-VIII

SUMMARY OF ORIGINAL DATA

DY-20 h_o = 0.2541

R_o	z	h
0	3.95	0.149
¼		.1555
½		.171
1	3.76	.187
2	3.39	.2065
3	2.98	.217
4	2.54	.2275
5	2.08	.2335
6	1.65	.2385
7	1.23	.243
8	0.86	.2445
9	0.50	.246
10	0.13	.2505

DY-21 h_o = 0.2549

R_o	z	h
0	2.26	.220
¼		.222
½		.223
1	2.18	.230
2	1.97	.239
3	1.75	.2425
4	1.45	.2445
5	1.21	.246
6	0.96	.246
7	0.74	.249
8	0.51	.2495
9	0.30	.2495
10	0.08	.2535

DY-27 h_o = 0.252

R_o	z	h	ds
0	1.24	.237	.0158
¼		.2395	
½		.240	
1	1.20	.244	
2	1.08	.247	.0101
3	0.95	.249	
4	.81	.2495	.0103
5	.65	.249	
6	.50	.2505	.0109
7	.39	.250	
8	.27	.2515	.0027
9	.14	.2515	
10	.01	.2520	.0202

All measurements are in inches.

R_o = Original radius

R = Radius after deformation

h_o = Original thickness

h = Thickness after distortion

z = Deflection

ds = Increase in distance between 2-inch punch marks

TABLE C-IX

SUMMARY OF ORIGINAL DATA

DY-30 h_o = 0.2384

R_o	z	h	R	ds
0	2.16	.220		.0383
¼		.218		
½		.2195		
1	2.08	.2215	1.023	
2	1.93	.227		.0411
3	1.70	.2305	3.026	
4	1.47	.232		.0345
5	1.28	.232	5.012	
6	0.99	.2325		.0320
7	0.77	.233	6.996	
8	0.54	.235		.0238
9	0.32	.237		
10	0.10	.2375		.0330

All measurements are in inches.

R_o = Original radius

R = Radius after deformation

h_o = Original thickness

h = Thickness after distortion

z = Deflection

ds = Increase in distance between 2-inch punch marks

TABLE C-X

SUMMARY OF ORIGINAL DATA

DY-31 h_o = 0.2430

R_o	z	h	ds	R
0	3.17		.1010	
¼		MDG		
½				
1	3.14	.2045		1.039
2	2.86	.213	.1152	
3	2.53	.2185		3.062
4	2.17	.2235	.0773	
5	1.84	.2265		5.051
6	1.49	.229	.0664	
7	1.14	.2305		7.012
8	0.80	.232	.0559	
9	0.47	.2335		8.976
10	0.14	.2385	.0577	

DY-32 h_o = 0.2316

R_o	R	z	ds	h
0		2.55	.0561	.202
¼				MDG
½				
1	1.020	2.46		.2075
2		2.26	.0606	.219
3	3.031	2.00		.221
4		1.70	.0480	.2235
5	5.027	1.45		.227
6		1.18	.0381	.2265
7	7.000	0.90		.2275
8		0.64	.0395	.2285
9	8.977	0.37		.230
10		0.11	.0442	.231

All measurements are in inches.

R_o = Original radius

R = Radius after deformation

h_o = Original thickness

h = Thickness after distortion

z = Deflection

ds = Increase in distance between 2-inch punch marks

TABLE C-XI

SUMMARY OF ORIGINAL DATA

DY-33 h_o = 0.2380

R_o	z	h	ds	R
0	2.59		.0554	
¼		MDG		
½				
1	2.53	.2075		
2	2.32	.2180	.0702	
3	2.05	.219		
4	1.77	.2265	.0527	
5	1.48	.230		
6	1.19	.229	.0472	
7	0.91	.231		
8	0.64	.232	.0363	
9	0.39	.233		
10	0.11	.2345	.0468	

NOT TAKEN

DY-34 h_o = 0.2391

R_o	R	z	ds	h
0		4.47	.4450	.147
¼				MDG
½				
1		4.30		.1735
2		3.93	.2600	.1875
3		3.49		.1995
4		2.99	.1347	.2075
5		2.50		.2145
6		2.02	.1063	.219
7		1.56		.2245
8		1.11	.0871	.2285
9		0.65		.2285
10		0.21	.0838	.232

NOT TAKEN

All measurements are in inches.

R_o = Original radius

R = Radius after deformation

h_o = Original thickness

h = Thickness after distortion

z = Deflection

ds = Increase in distance between 2-inch punch marks

TABLE C-XII

DATA FOR PLOTTING STRESS-STRAIN CURVES

MS (DY-1, 2, 3)

$\bar{\sigma} = F/A_o$	$\bar{\varepsilon} = \ell - \ell_o / \ell_o = A_o - A/A$
43,250	.01737
43,250	.02642
46,900	.03563
50,100	.04474
52,300	.05401
54,100	.07334
55,550	.08284
56,600	.09281
57,700	.11300
58,500	.12325
58,800	.14426
59,150	.15475
59,500	.17665
59,850	.19940
59,850	.22233
60,200	.24615
60,200	.27092
60,200	.32227
59,850	.45128
58,800	.65044
56,250	.94191

$\bar{\varepsilon}$ =Engineering Strain (in/in)

$\bar{\sigma}$ = Engineering Stress (#/in^2)

TABLE C-XIII

DATA FOR PLOTTING STRESS-STRAIN CURVES

STS (DY-7, 8, 9)

$\bar{\varepsilon}$	$\bar{\sigma}$
.0085	112,000
.0260	114,200
.0439	118,000
.0623	120,000
.0719	121,500
.1005	121,800
.1514	120,000
.2764	114,500
.4521	106,000
.8448	95,100

$\bar{\varepsilon}$ = Engineering Strain (in/in)

$\bar{\sigma}$ = Engineering Stress (#/in^2)

TABLE C-XIV

DATA FOR PLOTTING STRESS-STRAIN CURVES

MS (DY-16, 17, 18)

Specimen No. 1		Specimen No. 2		Specimen No. 3	
$\bar{\sigma}$	$\bar{\varepsilon}$	$\bar{\sigma}$	$\bar{\varepsilon}$	$\bar{\sigma}$	$\bar{\varepsilon}$
47491	.0080	47736		47736	
46756	.0045	47001	.0268	47736	.0268
52264	.0547	47368	.0453	52876	.0406
55936	.0646	52142	.0549	56548	.0596
58507	.0838	55814	.0741	59486	.0741
60710	.1003	58752	.0835	61322	.0888
62424	.1196	60588	.0987	62791	.1039
63403	.1355	62056	.1248	63892	.1248
64012	.1461	63158	.1350	64627	.1494
64749	.1792	63770	.1567	65361	.1622
65484	.1906	64994	.1732	65728	.1848
65851	.2138	65361	.1903	65728	.2077
66096	.2437	65728	.2132	65728	.2376
66218	.2448	66096	.2371	65728	.2738
66218	.3204	66096	.2616	65728	.3333
66218	.3817	66096	.2998	65728	.4104
65484	.4786	66096	.3531	64627	.5698
62913	.7173	66096	.4705	60955	.8867
57772	1.1645	63892	.6977	53611	1.3809
		59486	1.0080		
		51408	1.4691		

$\bar{\varepsilon}$ = Engineering Strain (in/in)

$\bar{\sigma}$ = Engineering Stress (#/in^2)

TABLE C-XV

DATA FOR PLOTTING STRESS-STRAIN CURVES

STS (DY-19, 20, 21)

Specimen No. 1		Specimen No. 2		Specimen No. 3	
$\bar{\sigma}$	$\bar{\varepsilon}$	$\bar{\sigma}$	$\bar{\varepsilon}$	$\bar{\sigma}$	$\bar{\varepsilon}$
96994	.0422	97796	.0042	97794	.0352
100052	.0213	101699	.0215	106003	.0624
104976	.0344	106520	.0438	109872	.1015
108333	.0477	109734	.0575	110576	.1744
110572	.0659	111571	.0762	107644	.2793
111915	.0847	112948	.0955	101312	.5037
112138	.1038	113407	.1252	92869	.7931
112138	.1286	110423	.2457	77157	1.4130
110795	.1752	104224	.4436		
106543	.3147	95730	.7309		
99828	.5270	84366	1.1664		
94008	.8573	68871	1.9123		
78676	1.4300				

$\bar{\varepsilon}$ = Engineering Strain (in/in)

$\bar{\sigma}$ = Engineering Stress (#/in^2)

TABLE C-XVI

DATA FOR STRESS-STRAIN CURVES

STS (DY-27, 28, 29)

Specimen No. 1		Specimen No. 2	
$\bar{\sigma}$	$\bar{\varepsilon}$	$\bar{\sigma}$	$\bar{\varepsilon}$
110,684		110,953	
113,010	.0261	112,862	.0265
114,172	.0351	115.725	.0353
118,357	.0533	119,304	.0447
120,915	.0816	121,690	.0730
122,078	.1313	122,645	.1437
117,660	.2535	116,918	.2822
109,986	.4400	108,567	.5098
99,406	.7677	97,830	.8464
85,455	1.2500	79,934	1.4361
68,015	2.4490		

$\bar{\varepsilon}$ = Engineering Strain (in/in)

$\bar{\sigma}$ = Engineering Stress (#/in^2)

TABLE C-XVII

DATA FOR STRESS-STRAIN CURVES

MS (DY-30-34)

Specimen No. 1		Specimen No. 2	
$\bar{\sigma}$	$\bar{\varepsilon}$	$\bar{\sigma}$	$\bar{\varepsilon}$
43,261		46,499	
43,261	.0396	47,676	.0097
44,144	.0396	47,087	.0396
47,970	.0434	52,090	.0499
51,207	.0708	55,327	.0603
54,150	.0925	58,859	.0816
55,327	.1148	59,742	.0980
56,799	.1378	61,213	.1148
57,682	.1615	61,802	.1326
57,976	.1859	62,979	.1495
59,153	.2111	63,273	.1736
59,448	.2372	63,568	.1984
59,742	.2641	64,009	.2241
59,742	.2919	64,156	.2530
59,742	.3655	64,156	.2919
59,742	.4970	64,156	.3855
57,388	.7331	63,569	.5329
52,973	1.116	59,448	.8008
44,144	1.907	52,090	1.374

$\bar{\varepsilon}$ = Engineering Strain (in/in)

$\bar{\sigma}$ = Engineering Stress (#/in^2)

TABLE C-XVIII

DATA FOR PLOTTING STRESS-STRAIN CURVES

(DY-10, 11, 12)
CRS

$\bar{\sigma}$	$\bar{\varepsilon}$
45,700	.0334
48,300	.0420
50,850	.0508
53,400	.0686
56,200	.0777
58,100	.0962
60,650	.1151
62,900	.1248
64,500	.1346
66,100	.1546
67,700	.1647
69,100	.1760
70,500	.1856
71,100	.1961
72,800	.2179
73,700	.2289
74,400	.2401
75,500	.2515
76,200	.2629
77,200	.2746
78,150	.2984
79,100	.3106
79,800	.3229
80,400	.3354
81,000	.3481
81,700	.3610
82,300	.3740
82,700	.3873
83,200	.4007
83,500	.4144

$\bar{\varepsilon}$ = Engineering Strain (in/in)

$\bar{\sigma}$ = Engineering Stress (#/in^2)

TABLE C-XIX

DATA FOR PLOTTING STRESS-STRAIN CURVES

(DY-13, 14, 15)
HY-80

$\bar{\varepsilon}$	$\bar{\sigma}$	$\bar{\varepsilon}$	$\bar{\sigma}$	$\bar{\varepsilon}$	$\bar{\sigma}$
.03068	95,330	.03552	96,155	.03555	97,826
.04122	97,718	.04471	99,019	.044735	99,496
.06280	101,856	.11258	102,120	.06008	102,598
.09264	103,447	.16517	104,506	.10248	104,387
.18146	104,720	.26972	104,029	.19853	104,029
.38406	799,468	.40329	98,064	.40329	98,064
.77771	89,760	.74234	89,475	.74234	89,475
1.44128	75,118	1.24906	77,545	1.24987	77,306
2.69781	58,089	2.15716	62,036	2.15716	62,036
		2.8975	57,264	2.9651	56,667

$\bar{\varepsilon}$ = Engineering Strain (in/in)

$\bar{\sigma}$ = Engineering Stress (#/in^2)

TABLE C-XX

DATA FOR PLOTTING STRESS-STRAIN CURVES

HTS (DY-4, 5, 6)

$\bar{\varepsilon}$	$\bar{\sigma}$	$\bar{\varepsilon}$	$\bar{\sigma}$	$\bar{\varepsilon}$	$\bar{\sigma}$
.02770	64,914	.00945	66,642	.00949	65,560
.03720	67,130	.02876	68,045	.01912	66,835
.046703	72,474	.04864	72,956	.04886	72,216
.06649	76,254	.06909	76,744	.06942	75,331
.09515	78,210	.09015	79,129	.07993	78,163
.10750	80,295	.11185	81,093	.10141	80,145
.13983	81,599	.14560	82,075	.13486	81,278
.17359	82,120	.19303	82,777	.15802	82,128
.24581	82,772	.28353	82,777	.19410	82,411
.38186	82,120	.44801	81,654	.27148	82,836
.65092	78,731	.75008	77,165	.40250	82,836
1.0801	71,692	1.18722	69,448	.65043	78,588
1.76145	61,916	1.99760	57,803	.99684	71,366
2.2283	57,354			1.87463	60,604
				2.22539	56,356

$\bar{\varepsilon}$ = Engineering Strain (in/in)

$\bar{\sigma}$ = Engineering Stress ($\#/in^2$)

FIGURE C-I

Stress-Strain and E/V Curves For
DY-1 , DY-2 , DY-3 ,(Mild Steel)

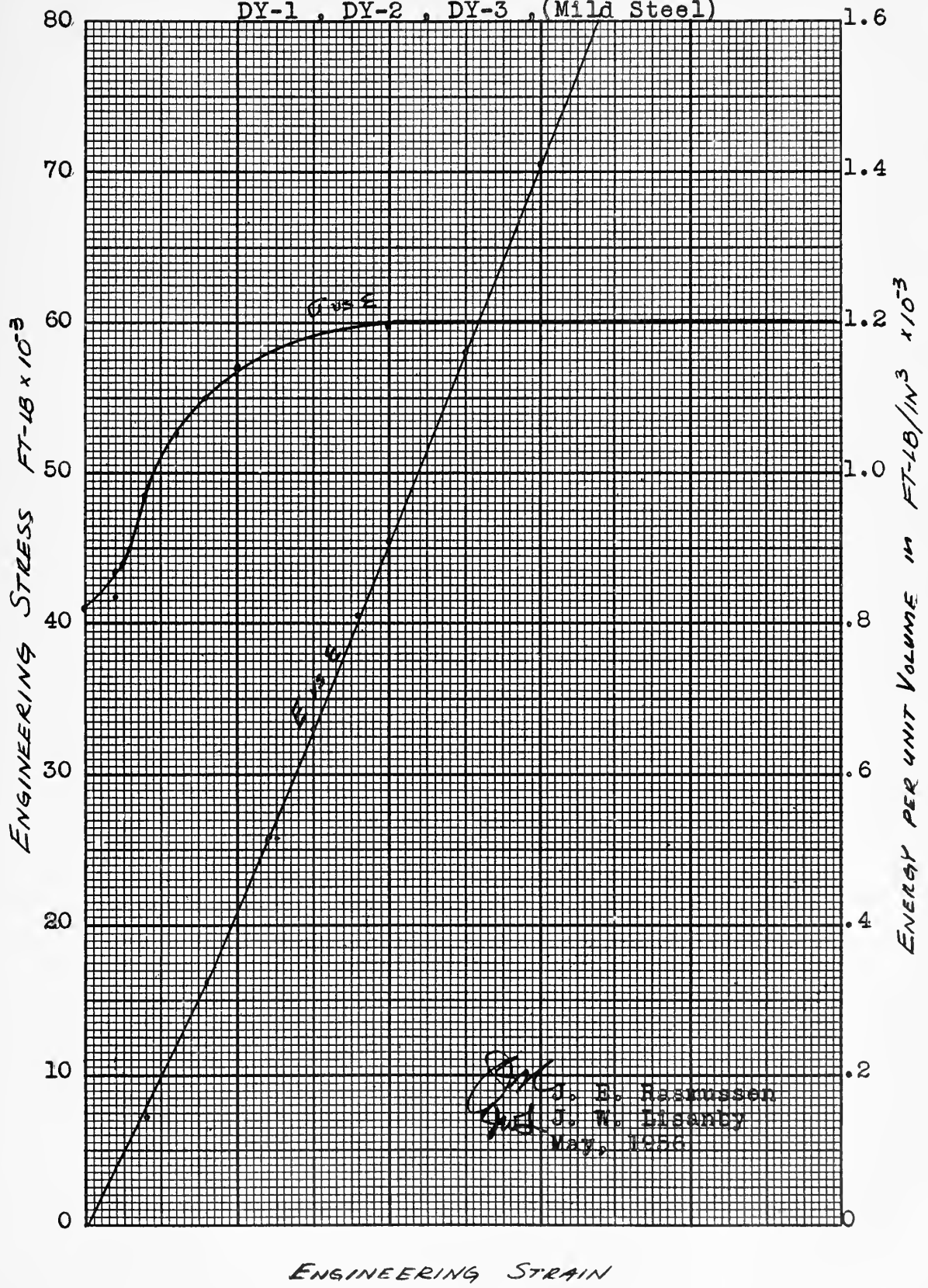

3. Material Analysis.

The following tests were conducted in accordance with the requirements of "The General Specifications for Inspection of Material (App. II--Metals)." The composition was determined through chemical analysis, the tensile properties through tensile tests, and the hardness through hardness tests.

In making the tensile tests, two specimens were cut from each sample. One of the two specimens was tested under conditions which gave a 1 to 500 extension ratio in a load-elongation curve, and the other under conditions which gave a 1 to 10 extension ratio. The two curves were obtained in order to show the shape of the load-elongation curve through both the initial yield and plastic deformation range.

Table XXI gives the chemical analysis. Table XXII lists the results of the tensile and hardness tests.

TABLE C-XXI-a

CHEMICAL ANALYSIS

	DY-1, 2, 3	DY-4, 5, 6	DY-7, 8, 9	DY-10, 11, 12	DY-13, 14, 15
	MS	HTS	STS	CRS	HY-80
Carbon (C), %	0.18	0.16	0.22	0.08	0.16
Phosphorus (P), %	0.02	0.02	0.02	0.02	0.02
Sulfur (S), %	0.03	0.03	0.03	0.01	0.02
Manganese (Mn), %	0.33	1.01	1.21	0.76	0.31
Molybdenum (Mo), %	0.06	0.07	0.08	0.52	0.18
Chromium (Cr), %	0.06	0.06	1.12	17.40	0.86
Nickel (Ni), %	0.11	0.10	2.70	10.00	2.05
Silicon (Si), %	0.07	0.22	0.25	0.44	0.22
Vanadium (V), %	None	None	None	----	None
Titanium (Ti), %	Trace	0.01	0.01	----	0.01
Copper, (Cu), %	0.23	0.04	0.03	----	0.05

TABLE C-XXI-b

CHEMICAL ANALYSIS

	DY-16, 17, 18	DY-19, 20, 21	DY-22, 23, 24
	MS	STS	MS
Manganese (Mn), %	0.35	0.33	0.40
Molybdenum (Mo), %	0.06	0.07	0.07
Chromium (Cr), %	0.06	1.20	0.10
Vanadium (V), %	None	None	----
Titanium (Ti), %	Trace	Trace	Trace
Copper (Cu), %	0.20	0.03	0.36
Nickel (Ni), %	0.13	2.60	0.14
Silicon (Si), %	0.06	0.23	0.06
Phosphorus (P), %	0.02	0.02	0.02
Sulfur (S), %	0.04	0.04	0.05
Carbon (C), %	0.24	0.21	0.20

TABLE C-XXII

RESULTS OF TENSILE AND HARDNESS TESTS

DY No.	Direction of Rolling	Tensile Strength, psi.	Yield (1) Strength, psi.	Elongation (2"), pct.	Hardness Rockwell B-Scale
1, 2, 3 MS	Long.	57,900	41,700	37.0	67-68.5
	"	58,800	44,200	34.0	
	Trans.	60,600	41,400	31.5	69-70
	"	59,800	44,200	33.0	
4, 5, 6 HTS	Long.	76,300	59,900	28.5	80-82
	"	75,800	57,200	29.0	
	Trans.	77,200	58,600	27.5	80-83
	"	77,700	57,400	26.0	
7, 8, 9 STS	Long.	121,300	109,200	17.5	24-25 (2)
	"	121,400	110,500	17.0	
	Trans.	122,500	112,300	15.0	24-25 (2)
	"	122,200	112,400	15.5	
10, 11, 12 CRES	Long.	79,800	32,200	59.0	86-88.5
	"	80,500	32,100	59.0	
	Trans.	80,300	31,900	60.0	87-89
	"	79,900	32,300	58.0	
13, 14 15 HY-80	Long.	101,800	88,000	20.5	96-97
	"	102,800	90,400	21.0	
	Trans.	106,900	95,700	18.0	99-100
	"	107,100	97,300	17.5	
16, 17, 18 MS	Long.	64,100	46,500	32.0	71.5-73.5
	"	64,300	47,100	29.5	
	Trans.	64,700	46,100	30.0	72.5-75
	"	64,500	45,700	29.0	
19, 20, 21 STS	Long.	107,800	90,600	21.0	97.5-98.5
	"	110,200	93,400	21.0	
	Trans.	113,900	101,200	14.0	99-100
	"	113,900	101,600	14.0	
22, 23, 24 MS	Long.	65,900	51,600	28.5	75-76
	"	66,700	52,100	30.0	
	Trans.	66,000	49,000	29.0	74-75
	"	65,400	48,800	28.5	

Footnotes: (1) Extension under load method: paragraph 47 (c), reference (b), 0.5 pct. extension taken from the load-elongation curve.

(2) Rockwell "C" scale.

APPENDIX D

SAMPLE CALCULATIONS

To provide continuity for the sample calculations, a full set will be given for one specific test, DY-7, beginning with the basic data and ending with the final value of total energy absorbed by the plate.

Test Plate DY-7

Initial thickness = 0.248 in.

h = thickness after deformation

TABLE D-1

Calculation of $\varepsilon_h = \frac{\Delta h}{h} = \frac{h_o - h}{h}$

R	ΔV	h	Δh	ε_h	$\int \sigma_h d\varepsilon_h$	ΔE_h
in	in^3	in	in	in/in	ft-#/in^3	ft-#
0.5	0.442	.2000	.0480	.240	2.400	1.061
1.0	0.785	.2090	.0390	.187	1.870	1.468
1.5	1.178	.2150	.0330	.153	1.530	1.802
2.0	1.571	.2210	.0270	.122	1.220	1.917
2.5	1.963	.2260	.0220	.097	0.960	1.884
3.0	2.356	.2280	.0198	.087	0.855	2.014
3.5	2.749	.2308	.0172	.075	0.732	2.012
4.0	3.142	.2325	.0155	.067	0.650	2.042
4.5	3.534	.2345	.0135	.058	0.560	1.979
5.0	3.927	.2360	.0120	.051	0.490	1.924
5.5	4.320	.2370	.0110	.046	0.440	1.901
6.0	4.712	.2380	.0100	.042	0.400	1.885
6.5	5.105	.2398	.0082	.034	0.325	1.659
7.0	5.498	.2415	.0065	.027	0.255	1.402
7.5	5.890	.2430	.0050	.021	0.200	1.178
8.0	6.283	.2435	.0045	.018	0.170	1.068
8.5	6.676	.2430	.0050	.021	0.200	1.335
9.0	7.069	.2425	.0055	.023	0.220	1.555
9.5	7.461	.2450	.0030	.012	0.110	0.821
10.0	3.874	.2480	0	0	0	0

From Table D-1, the increments of energy may be summed to give:

$\Sigma \Delta E_h$ = 30,907 foot pounds

To this energy must be added the energy which went into bending. This is evaluated from the expression for bending given in Chapter I.

$$E_B = 4\pi M_o \theta D/2 = \pi \sigma_{yp} h^2 \theta D/2 \qquad (18)$$

Test Plate DY-7

$D/2 = 10$ in $= 0.833$ ft.

$h = 0.25$ in

$[\sigma_{yp}]$ edge $= 112{,}600$

$\theta = 15^\circ = 0.262$ rad.

$E_B = \pi \times 112{,}600 \times 0.0625 \times 0.262 \times 0.833$

$E_B = 4{,}820$ foot pounds

Therefore, the total energy of deformation is:

$E_T = E_h + E_B = 30{,}907 + 4{,}820 = 35{,}727$ foot pounds.

APPENDIX E

DETAILS OF STATISTICAL ANALYSIS

The use of a rigorous statistical analysis for this problem involves the knowledge of several basic theorems of statistics which deal with the distribution of a function of a variable. For clarity, these theorems are quoted at the outset. The reader is referred t o various texts on statistical analysis for the proof and discussion of such theorems (7, 14, 20).

NOMENCLATURE

x = Specific value of the variable

n = Size of sample taken from any given population of the variable

$\bar{x}$ = Arithmetic mean of a sample

$\bar{X}$ = Arithmetic mean of a total population

σ^2 = Variance of a total population

s^2 = Variance of a sample

N = Symbol denoting normal distribution of a variable

χ^2 = Symbol denoting a specific distribution

1. Statistical Theorems.

The following theorems are quoted from Hoel (14) to be used in this solution:

Theorem II: If x is normally distributed with variance σ^2 and s^2 is the sample variance based on a random sample of size n, then ns^2/σ^2 has χ^2 distribution with n - 1 degrees of freedom.

Theorem III: If χ_1^2 and χ_2^2 possess independent χ^2 distributions with ν_1 and ν_2 degrees of freedom respectively, then $\chi_1^2 + \chi_2^2$ will possess a χ^2 distribution with $\nu_1 + \nu_2$ degrees of freedom.

Theorem IV: If u is normally distributed with zero mean and unit variance and v^2 has a χ^2 distribution with ν degrees of freedom and if u and v are independently distributed, then the variable $t = \frac{u\sqrt{\nu}}{v}$ has Student's t distribution with ν degrees of freedom. By the use of these three theorems, the full solutions of the problems considered in Chapter IV may be accomplished.

2. Derivation of Confidence Limits for the Difference of the Means.

To compute confidence limits for the average difference of the sample mean, the sample variance of the difference function must first be evaluated to the best possible estimate. This is done by use of the statistical theorem which expresses the resulting variance, σ_R, for a function $x = c_1x_1 + c_2x_2 + c_3x_3 + \cdots c_nx_n$ as $\sigma_R = \sqrt{\sum_1^n c_n^2\sigma^2}$, where σ is considered constant for each value x_n. Thus, to apply this theorem to the function of the difference of the

means, $\bar{x}_{HY} - \bar{x}_{MS}$, the expression must be expanded to a sum of individual values of x. This is done as follows:

Let the various standoff values be represented by a = 1, 2, 3, ----α. Let the mean value, $\bar{x}$, of all mild steel energies at any one standoff be represented by $\bar{x}_{ma}$ and for the high yield steels, $\bar{x}_{HY}$. Let β_m and β_H represent the number of test points at each standoff for mild steel and high yield steel, respectively. The difference of the means may then be expressed by:

$$\bar{x}_{Ha} - \bar{x}_{ma} = \frac{\sum_{a=1}^{\alpha} \left[\beta_H \bar{x}_{ma} - \frac{\beta_H \bar{x}_{Ha}}{\beta_H + \beta_m} - \frac{\beta_m \bar{x}_{ma}}{\beta_H + \beta_m} \right]}{\sum_{a=1}^{\alpha} \beta_H} - \frac{\sum_{a=1}^{\alpha} \left[\beta_m \bar{x}_{ma} - \frac{\beta_H \bar{x}_{Ha}}{\beta_H + \beta_m} - \frac{\beta_m \bar{x}_{ma}}{\beta_H + \beta_m} \right]}{\sum_{a=1}^{\alpha} \beta_m} \quad \text{(E-1)}$$

This may be written as:

$$\bar{x}_H - \bar{x}_m = \frac{1}{\sum_{a=1}^{\alpha} \beta_H} \sum_{a=1}^{\alpha} \left(\beta_H - \frac{\beta_H}{\beta_H + \beta_m} + \frac{\sum \beta_H}{(\beta_H + \beta_m) \sum_{a=1}^{\alpha} \beta_m} \right) \bar{x}_{Ha}$$

$$+ \frac{1}{\sum_{a=1}^{\alpha} \beta_m} \sum_{a=1}^{\alpha} \left(\beta_m - \frac{\beta_m}{\beta_m + \beta_H} + \frac{\sum \beta_m}{(\beta_m + \beta_H) \sum_{a=1}^{\alpha} \beta_H} \right) \bar{x}_{ma} \quad \text{(E-2)}$$

$$\bar{x}_H - \bar{x}_m = \frac{1}{\sum_{a=1}^{\alpha} \beta_H} \sum_{a=1}^{\alpha} \left[\frac{(\beta_H \beta_m + \beta_H^2 - \beta_H) \sum_{a=1}^{\alpha} \beta_m + \sum_{a=1}^{\alpha} \beta_H}{(\beta_H + \beta_m) \sum_{a=1}^{\alpha} \beta_m} \right] \bar{x}_{Ha}$$

$$+ \frac{1}{\sum_{a=1}^{\alpha} \beta_m} \sum_{a=1}^{\alpha} \left[\frac{(\beta_m \beta_H + \beta_m^2 - \beta_m) \sum_{a=1}^{\alpha} \beta_H + \sum_{a=1}^{\alpha} \beta_m}{(\beta_m + \beta_H) \sum_{a=1}^{\alpha} \beta_H} \right] \bar{x}_{ma} \quad \text{(E-3)}$$

Applying the theorem we may represent the resulting variance, σ_R, of the function $\bar{x}_H - \bar{x}_m$, as:

$$\sigma_R = \sigma \sqrt{\sum_{a=1}^{\alpha} \left[\frac{1}{\sum \beta_H} \frac{(\beta_H \beta_m + \beta_H^2 - \beta_H) \sum \beta_m + \sum \beta_H}{(\beta_H + \beta_m) \sum \beta_m} \right]^2 \frac{1}{\beta_H} + \left[\frac{1}{\sum \beta_m} \frac{(\beta_m \beta_H + \beta_m^2 - \beta_m) \sum \beta_H + \sum \beta_m}{\beta_m + \beta_H \sum \beta_H} \right]^2 \frac{1}{\beta_m}}$$

This radical is then evaluated by Table E-1. And the result is given as, $\sigma_R = 0.395\sigma$.

The remainder of the equation $t = \frac{u\sqrt{\nu}}{v}$ may be evaluated as:

$$\sqrt{\nu} = \sqrt{n_1 - 2 + n_2 - 2 + n_3 - 2 + n_4 - 2} =$$

$$\sqrt{(5 - 2)+(6 - 2)+(5 - 2)+(4 - 2)} = \sqrt{12} = 3.47$$

$v = \frac{1}{\sigma}\sqrt{\sum_{m=1}^{m}(x_m-\bar{x}_m)^2_{ms}+\sum_{m=1}^{n}(x_m-\bar{x}_m)^2_{HY}}$ where the summations under the radical may be taken from Tables E-2 and E-3.

$v = \frac{1}{\sigma}\sqrt{14.815 + 24.879} = 6.31/\sigma$, and $t = 2.18$ based on $\nu = 12$ and 95% confidence.

The function u is now

$$u = \frac{[(\bar{x}_{HY} - \bar{x}_{ms}) - (\bar{X}_{HY} - \bar{X}_{ms})]}{\sigma_R}$$

The final expression is then:

$$t = \frac{[(\bar{x}_{HY} - \bar{x}_{ms}) - (\bar{X}_{HY} - \bar{X}_{ms})]}{\sigma_R} \times \frac{\sqrt{\nu}}{v} \qquad \text{(E-4)}$$

TABLE E-1

CALCULATION OF σ_R

a	1	2	3	4	
β_m	3	3	2	3	Σ 11
β_m^2	9	9	4	9	
β_H	2	3	3	1	Σ 9
β_H^2	4	9	9	1	
$\beta_H \beta_m$	6	9	6	3	
$\beta_H + \beta_m$	5	6	5	4	
$\beta_H\beta_m + \beta_m^2 - \beta_m$	12	15	8	9	
$\beta_m\beta_H + \beta_H^2 - \beta_H$	8	15	12	3	
$(\sigma_R/\sigma)^2$	.0385	.0487	0410	0278	Σ= 0.156

$$\sigma_R = \sigma\sqrt{.156} = \sigma(0.395)$$

2. Derivation of Confidence Limits for the Curve of the Mean.

a. By use of Theorem II and standard symbols, $\frac{\sum(x_1-\bar{x}_1)^2}{\sigma^2}$ has χ^2 distribution with $(n_1 - 1)$ degrees of freedom, where all samples are assumed to have the same variance .

b. By use of Theorem III this is extended to,

$$V^2 = \left(\frac{\sum(x_1-\bar{x}_1)^2}{\sigma^2} + \frac{\sum(x_2-\bar{x}_2)^2}{\sigma^2} + \frac{\sum(x_3-\bar{x}_3)^2}{\sigma^2} + \frac{\sum(x_4-\bar{x}_4)^2}{\sigma^2}\right) \qquad \text{(E-5)}$$

has χ^2 distribution with $\nu = \left[(n_1-1)+(n_2-1)+(n_3-1)+(n_4-1)\right]$ degrees of freedom.

In all equations the subscripts 1, 2, 3, 4 refer to a sample of values taken from standoff distances of 4, 5, 6, and 7 feet respectively.

c. The final expression may be derived by use of Theorem IV, which gives:

$$t = \frac{(\bar{x}_1 - \bar{X}_1)}{\sigma / \sqrt{n_1}} \times \frac{\sqrt{\nu}}{V} \qquad \text{(E-6)}$$

which may be cleared and expanded to give:

$$(\bar{x}_1 - \bar{X}_1) = \frac{\pm t\sqrt{\sum(x_1-\bar{x}_1)^2 + \sum(x_2-\bar{x}_2)^2 + \sum(x_3-\bar{x}_3)^2 + \sum(x_4-\bar{x}_4)^2}}{\sqrt{\nu} \times \sqrt{n_1}}$$

where Student's t is based on ν degrees of freedom and 95% probability. This last expression may then be evaluated for mild steel at each standoff and this calculation is completed in Table E-2.

d. The high yield steels are treated in exactly the same manner in Table E-3.

TABLE E-2

COMPUTATION FOR THE STATISTICAL

ANALYSIS OF RESULTS FOR MILD STEEL

n	x Energy Values	$\bar{x}$ Mean	$(x-\bar{x})^2$	$\Sigma(x-\bar{x})^2$	$\sqrt{\nu}$	$\sqrt{n}$	t	$(\bar{x}_1 - \bar{X}_1)$
n_1	37600 37600 34800	36,667	.871 .871 3.486	5.228	2.646	1.732	2.36	1.980
n_2	21410 21300 18230	20,313	1.203 .974 4.339	6.516	2.646	1.732	2.36	1.980
n_3	11890 13060	12,475	.342 .342	.684	2.646	1.414	2.36	2.430
n_4	9850 8170 7800	8,607	1.545 .191 .651	2.387	2.646	1.732	2.36	1.980
			$\Sigma =$	14.815				

TABLE E-3

COMPUTATION FOR THE STATISTICAL ANALYSIS

OF RESULTS FOR HIGH YIELD STEELS

n	x Energy Values	$\bar{x}$ Mean	$(x-\bar{x})^2$	$\sum(x-\bar{x})^2$	$\sqrt{\nu}$	$\sqrt{n}$	t	$(\bar{x} - \bar{X})$
n_1	35450 35700	35,575	.015625 .015625	.03125	2.236	1.414	2.57	4.050
n_2	20200 24180 22500	22,293	4.381 3.561 .043	7.985	2.236	1.732	2.57	3.310
n_3	17800 12270 13500	14,523	10.740 5.076 1.047	16.863	2.236	1.732	2.57	3.310
n_4	7350	7,350	0	0	2.236	1	2.57	5.740
				$\sum =$ 24.879				

APPENDIX F

ORIGINAL DATA

All original data is on file at the Underwater Explosion Research Division, Norfolk Naval Shipyard, Portsmouth, Virginia. Calculations for the thesis were based on values for one average radii, and such averages are included as Appendix C. To demonstrate the form in which all original data was recorded, two sample plates, DY-7 and DY-21, are presented with the original, unaveraged values. DY-7 represents a plate in which the variance in the data for the four radii is large. DY-21 represents the more common test in which values for all four radii are in close agreement.

ORIGINAL DATA

DY-7

STS, Standoff = 4'

Deflections

TABLE F-1

	Direction of Roll			Transverse		
R	Before	After	Z (in)	Before	After	Z (in)
12	3.73	3.73		3.70	3.66	
11	3.72	3.72		3.69	3.65	
10	3.72	3.83	0.11	3.69	3.82	0.13
9	3.72	4.15	0.43	3.68	4.11	0.39
8	3.72	4.43	0.71	3.67	4.38	0.65
7	3.73	4.75	1.02	3.67	4.68	0.95
6	3.73	5.09	1.36	3.67	4.98	1.25
5	3.73	5.42	1.69	3.67	5.33	1.60
4	3.74	5.79	2.05	3.67	5.67	1.94
3	3.73	6.14	2.41	3.67	6.04	2.31
2	3.73	6.47	2.74	3.67	6.38	2.65
1	3.73	6.75	3.02	3.67	6.67	2.94
c	3.73	6.85	3.12	3.67	6.78	3.05
1	3.73	6.71	2.98	3.67	6.64	2.91
2	3.73	6.41	2.68	3.67	6.34	2.61
3	3.72	6.04	2.32	3.68	6.03	2.32
4	3.72	5.68	1.96	3.68	5.68	1.97
5	3.72	5.33	1.61	3.68	5.30	1.59
6	3.71	5.00	1.29	3.69	4.95	1.26
7	3.71	4.69	0.98	3.69	4.62	0.93
8	3.71	4.39	0.68	3.69	4.31	0.58
9	3.71	4.10	0.39	3.70	4.01	0.31
10	3.71	3.81	0.10	3.70	3.72	0.02
11	3.72	3.72		3.70	3.66	
12	3.72	3.72	(1)	3.70		(1)

(1) Includes small correction for any initial bulge in the plate at the backing shoulder.

ORIGINAL DATA

DY-7

STS, Standoff = 4'

Thickness

TABLE F-2

R	h (radius #1)	h (radius #2)	h (average)
c	0.194		0.194
$\frac{1}{4}$	0.1960	0.1925	0.1942
$\frac{1}{2}$	0.2025	0.1995	0.2010
1	0.2085	0.2060	0.2072
2	0.2215	0.2205	0.2210
3	0.2295	0.2270	0.2282
4	0.2325	0.2320	0.2322
5	0.2370	0.2350	0.2360
6	0.2390	0.2370	0.2380
7	0.2425	0.2410	0.2417
8	0.2440	0.2435	0.2437
9	0.2435	0.2420	0.2427
10	0.2510	0.2440	0.2490
11	0.2490	0.2475	
12	0.2485	0.2475	

All readings are in inches.

ORIGINAL DATA

DY-7

STS, Standoff = 4'

Radial Strain by Punch Marks

TABLE F-3

	Direction of Roll			Transverse		
	Before	After	ΔS	Before	After	ΔS
11-9	1.9976	2.0750	2.0774	1.9986	2.0750	2.0764
9-7	1.9960	2.0413	2.0453	1.9985	2.0413	2.0428
7-5	1.9970	2.0555	2.0585	1.9990	2.0546	2.0556
5-3	1.9988	2.0813	2.0825	1.9967	2.0727	2.0760
3-1	1.9988	2.1108	2.1120	1.9969	2.1095	2.1126
1-c-1	1.9964	2.1875	2.1911	1.9962	2.1875	2.1913
1-3	1.9971	2.1101	2.1130	1.9958	2.1092	2.1134
3-5	1.9948	2.0714	2.0766	1.9982	2.0780	2.0798
5-7	1.9965	2.0511	2.0546	1.9963	2.0531	2.0568
7-9	1.9946	2.0381	2.0435	1.9959	2.0398	2.0439
9-11	1.9979	2.0800	2.0821	1.9967	2.0650	2.0683

ORIGINAL DATA

DY-21

STS, Standoff = 5'

Deflections

TABLE F-4

	Direction of Roll			Transverse		
R	Before	After	Z (in)	Before	After	Z (in)
12	3.70	3.68		3.68	3.66	
11	3.69	3.68		3.66	3.64	
10	3.68	3.78	0.10	3.65	3.73	0.08
9	3.68	3.99	0.29	3.65	3.96	0.31
8	3.68	4.21	0.51	3.64	4.18	0.54
7	3.67	4.44	0.73	3.64	4.41	0.77
6	3.67	4.69	0.98	3.63	4.65	1.00
5	3.66	4.94	1.22	3.63	4.91	1.26
4	3.66	5.20	1.48	3.62	5.12	1.46
3	3.66	5.46	1.76	3.62	5.41	1.75
2	3.66	5.69	1.99	3.61	5.65	1.98
1	3.66	5.90	2.20	3.61	5.84	2.17
c	3.66	5.97	2.27	3.61	5.93	2.26
1	3.66	5.88	2.18	3.62	5.85	2.19
2	3.65	5.65	1.94	3.62	5.62	1.96
3	3.65	5.40	1.71	3.62	5.34	1.68
4	3.65	5.15	1.46	3.62	5.08	1.42
5	3.65	4.89	1.20	3.62	4.83	1.17
6	3.65	4.64	0.95	3.62	4.59	0.93
7	3.65	4.40	0.73	3.63	4.37	0.72
8	3.65	4.18	0.51	3.64	4.14	0.50
9	3.66	3.96	0.30	3.63	3.93	0.29
10	3.66	3.74	0.08	3.64	3.73	0.09
11	3.68	3.65		3.65	3.63	
12	3.68	3.67		3.66	3.65	
			(1)			(1)

(1) Includes small correction for any initial bulge in plate at the backing shoulder.

ORIGINAL DATA

DY-21

h_o = 0.2599 (in)

STS, Standoff = 5'

Thickness

TABLE F-5

R	h (radius #1)	h (radius #2)	h (average)
c	0.220		0.220
$\frac{1}{4}$	0.221	0.223	0.222
$\frac{1}{2}$	0.224	0.222	0.223
1	0.228	0.232	0.230
2	0.237	0.241	0.239
3	0.242	0.243	0.2425
4	0.243	0.246	0.2445
5	0.246	0.246	0.246
6	0.245	0.247	0.246
7	0.248	0.250	0.249
8	0.248	0.251	0.2495
9	0.250	0.249	0.2495
10	0.253	0.254	0.2535
11	0.253	0.255	
12	0.254	0.257	

All readings are in inches.

APPENDIX G

BIBLIOGRAPHY

1. Belsheim, R. O., DELAYED YIELD TIME EFFECT IN MILD STEEL UNDER OSCILLATING AXIAL LOADS, Naval Research Laboratory Report 4312 of March, 1954.

2. Clark, D. S., THE BEHAVIOR OF METALS UNDER DYNAMIC LOADING, Edward deMille Campbell Memorial Lecture, Thirty-fifth Annual Convention of The American Society for Metals, 1953.

3. Clark, D. S. and Wood, D. S., THE TIME DELAY FOR THE INITIATION OF PLASTIC DEFORMATION AT RAPIDLY APPLIED CONSTANT STRESS, "Proceedings of the American Society for Testing Metals," Volume 49, 1949.

4. Clark, D. S. and Wood, D. S., DELAYED YIELD IN ANNEALED STEELS OF VERY LOW CARBON AND NITROGEN CONTENT, A Paper Presented before the Thirty-third Annual Convention of the American Society for Metals, 1951.

5. Clark, D. S., Wood, D. S. and Vreeland, T. Jr., A STUDY OF THE MECHANISM OF THE DELAYED YIELD PHENOMENON, A Paper Presented before the Eighth Western Metal Congress of the American Society for Metals, 1953.

6. Cole, R. H., UNDERWATER EXPLOSIONS, Princeton University Press, Princeton, New Jersey, 1948, 437 pp.

7. Dixon, W. J. and Massey, F. J. Jr., INTRODUCTION TO STATISTICAL ANALYSIS, McGraw-Hill Inc., New York, 1951, 370 pp.

8. Gleyzal, A. N., PLASTIC STRAIN AND DEFLECTION TESTS ON CLAMPED CIRCULAR STEEL PLATES TWENTY INCHES IN DIAMETER, David Taylor Model Basin Report R-142, 1944.

9. Gleyzal, A. N., PLASTIC DEFORMATION AND ENERGY ABSORPTION OF A THIN RECTANGULAR PLATE UNDER HYDROSTATIC PRESSURE, David Taylor Model Basin Report R-280, 1945.

10. Gleyzal, A. N., PLASTIC DEFORMATION OF A THIN CIRCULAR PLATE UNDER PRESSURE, David Taylor Model Basin Report 532, 1946.

11. Gleyzal, A. N., PROGRESS REPORT ON UNDERWATER EXPLOSION RESEARCH--PLASTIC DEFORMATION OF AND ABSORPTION OF THIN CIRCULAR PLATES UNDER NORMAL LOADING, David Taylor Model Basin Report R-248, 1944.

12. Hetenyi, M., HANDBOOK OF EXPERIMENTAL STRESS ANALYSIS, John Wiley and Sons, Inc., New York, 1950.

BIBLIOGRAPHY

(continued)

13. Hill, R., PLASTICITY, Oxford-at-the-Clarendon Press, London, 1950, 354 pp.

14. Hoel, P. G., INTRODUCTION TO MATHEMATICAL STATISTICS, John Wiley and Sons, Inc., New York, 1947, 258 pp.

15. Kennard, E. H., EFFECT OF A PRESSURE WAVE ON A PLATE OR DIAPHRAGM, David Taylor Model Basin Report 527, 1944.

16. Keil, A. H., PRELIMINARY COMMENTARIES ON PLASTIC DEFORMATION OF RECTANGULAR PLATES UNDER DYNAMIC LOADING, U. S. Navy Underwater Explosions Research Division Confidential Report 1-47, 1947.

17. Keil, A. H., ADDITIONAL COMMENTARIES ON PLASTIC DEFORMATION OF RECTANGULAR PLATES UNDER DYNAMIC LOADING, U. E. R. D. Confidential Report 2-48.

18. Keil, A. H., INFORMATION ON DELAYED YIELD EFFECTS, Unpublished File (Confidential) U. E. R. D. F-17-55, 1955.

19. Massard, J. M., RAPID LOADING TESTS OF HY-80 SPECIMENS, Unpublished Test Data Gathered at the University of Illinois Nobs 62250.

20. Moroney, M. J., FACTS FROM FIGURES, Penquin Books, Baltimore, 1951, 472 pp.

21. Roark, R. J., FORMULAS FOR STRESS AND STRAIN, McGraw-Hill Inc., New York, 1954, 381 pp.

22. Schauer, H. M., PLASTIC DEFORMATION OF RECTANGULAR PLATES UNDER DYNAMIC LOADING, U. S. Navy Underwater Explosions Research Division Confidential Report 4-50, 1950.

23. Smith, G. V., PROPERTIES OF METALS AT ELEVATED TEMPERATURES, McGraw-Hill Book Co., New York, 1950, 399 pp.

24. Taylor, Sir G. I., THE TESTING OF MATERIALS AT HIGH RATES OF LOADING, "Journal of the Institute of Civil Engineers," Session 1945-46.

23027

Thesis
L68

Lisanby
The relative strengthening of steels at the high strain-rates of underwater explosive loading.